International Symposium on Fractional PDEs: Theory, Numerics and Applications
June 3 -5, 2013

Salve Regina University, Newport, RI

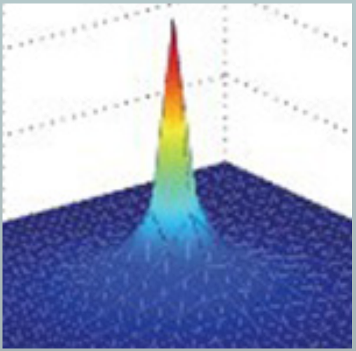

Organizing Committee

George Karniadakis

Jan Hesthaven

Local Organizers

Ernest Rothman, Salve Regina University

Ms. Madeline Brewster, Brown University

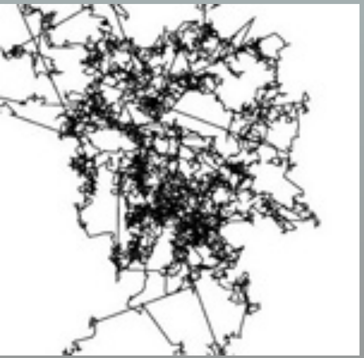

Sponsors

Air Force Office of Scientific Research

US Army Research Office

Department of Energy/Pacific Northwest National Lab

Théorie Analytique de la Chaleur,1822

Introduction
SECTION 1. Statement of the Object of the Work

"The effects of heat are subject to constant laws which can not be discovered without the aid of mathematical analysis. The object of the theory which we are about to explain is to demonstrate these laws; it reduces all physical researches on the propagation of heat, to problems of the integral calculus whose elements are given by experiment."

Joseph Fourier

1768 -1830

Let *v* be the actual temperature of the point (*x,y,z*). The following equation represents the movement of heat in the interior of bodies.

$$\frac{dv}{dt} = \frac{K}{CD}\left(\frac{d^2v}{dx^2} + \frac{d^2v}{dy^2} + \frac{d^2v}{dz^2}\right)$$

K – thermal conductivity
C – specific heat
D – density

Théorie Analytique de la Chaleur,1822

Introduction
SECTION 1. Statement of the Object of the Work

"The effects of heat are subject to constant laws which can not be discovered without the aid of mathematical analysis. The object of the theory which we are about to explain is to demonstrate these laws; it reduces all physical researches on the propagation of heat, to problems of the integral calculus whose elements are given by experiment."

Joseph Fourier

1768 -1830

Let *v* be the actual temperature of the point (*x,y,z*). The following equation represents the movement of heat in the interior of bodies.

$$\frac{dv}{dt} = \frac{K}{CD}\left(\frac{d^2v}{dx^2} + \frac{d^2v}{dy^2} + \frac{d^2v}{dz^2}\right)$$

K – thermal conductivity
C – specific heat
D – density

Entropy as a Measure of Non-Gaussian Diffusion in Porous Tissues Viewed using MRI

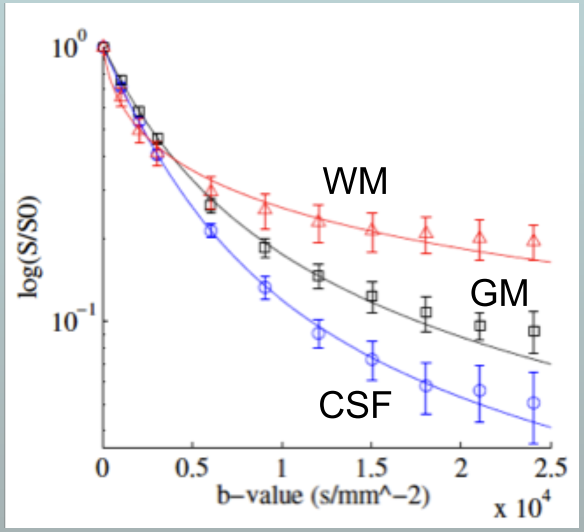

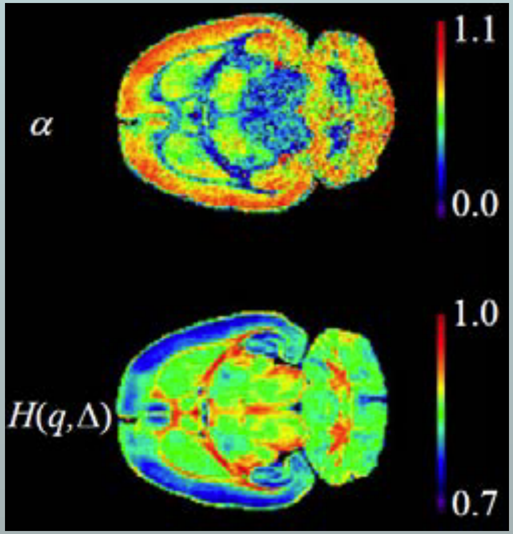

R.L Magin, C. Ingo, *Dept. of BioE, University of Illinois at Chicago*
L. Colon-Perez, *Dept. of Physics, University of Florida*
T.H. Mareci, *Dept. of Biochemistry, University of Florida*
T. Barrick, St. George's Hospital, University of London
A. Hanyga, Warsaw Poland

Outline

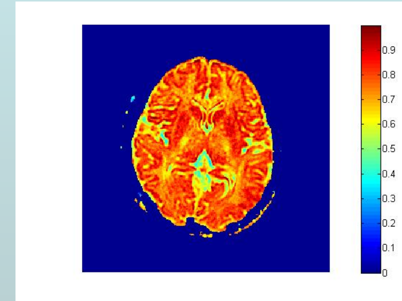

- Diffusion weighted MRI and DTI are used to detect neurodegenerative, malignant and ischemic diseases.

- The correlation between disease and tissue structure relies on pulse sequences that probe relaxation times and molecular diffusion, typically with $S=S_0\exp(-bD)$.

- Recent studies focus on anomalous diffusion, a process in which the NMR signal decays via $S=S_0E_\alpha(-D_{\alpha,\beta}q^\beta\Delta^\alpha)$, where α and β are fractional measures of tissue complexity.

- In this presentation, I will describe a model of anomalous diffusion derived using fractional calculus that uses α, β and entropy as measures of tissue complexity.

Diffusion in NMR and MRI

Diffusion weighted MR imaging (DWI) and tensor imaging (DTI) are a powerful tools for characterizing normal and abnormal brain structures

DWI can detect stroke and tumors, while DTI can readily detect changes in anisotropic diffusion in the white matter.

Bloch Equatıon

$$\frac{\partial \vec{M}(\vec{r},t)}{\partial t} = \gamma \vec{M}(\vec{r},t) \times \vec{B} + \frac{M_0 - M_z}{T_1}\hat{z} - \frac{M_x \hat{x} + M_y \hat{y}}{T_2}$$

Brain MRI at 3 T

MRI Signal Processing

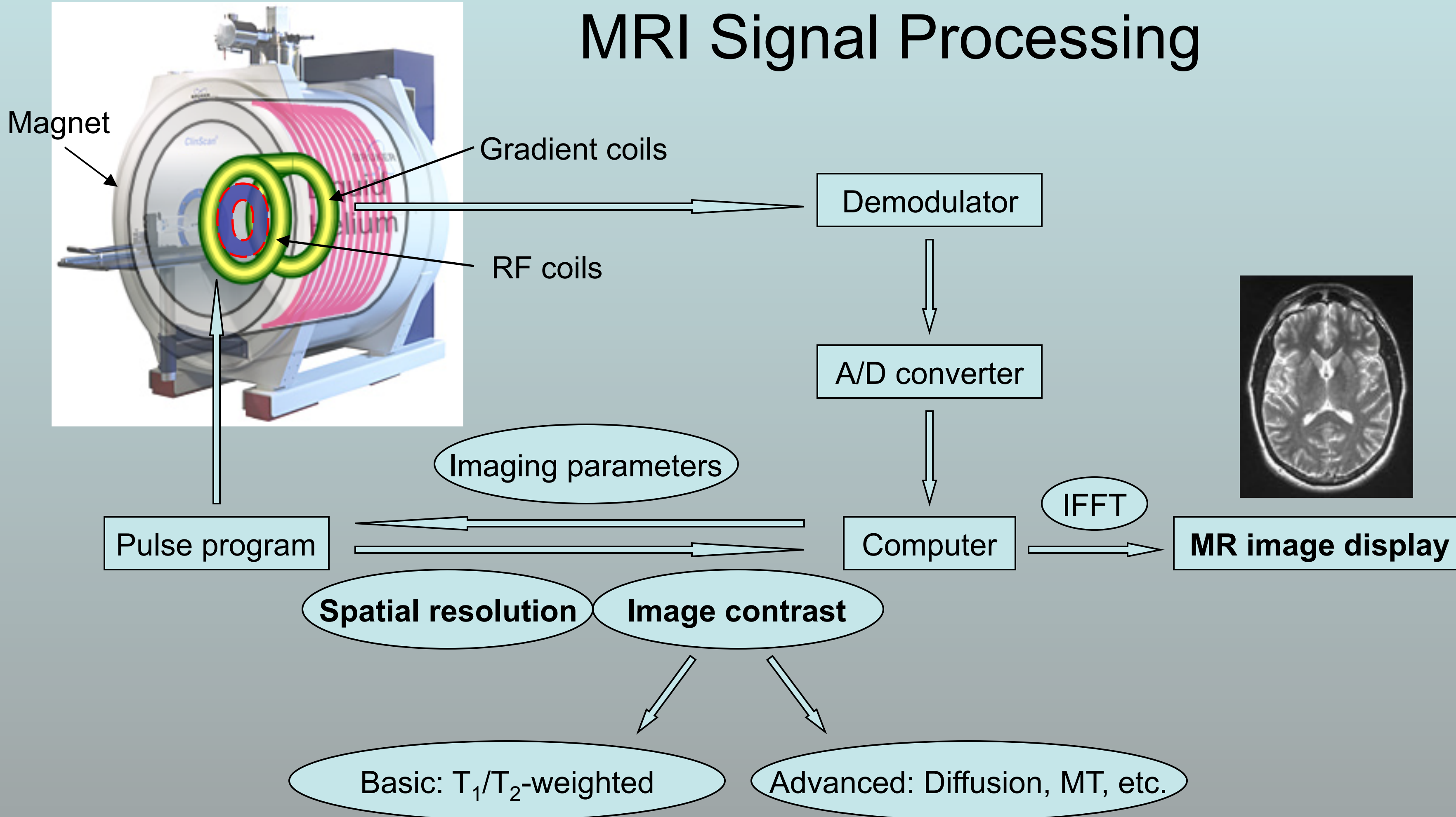

MR images thus provide quantitative spatial maps of tissue parameters, T1, T2 and the diffusion constant, D.

Spin Echo Pulse Program

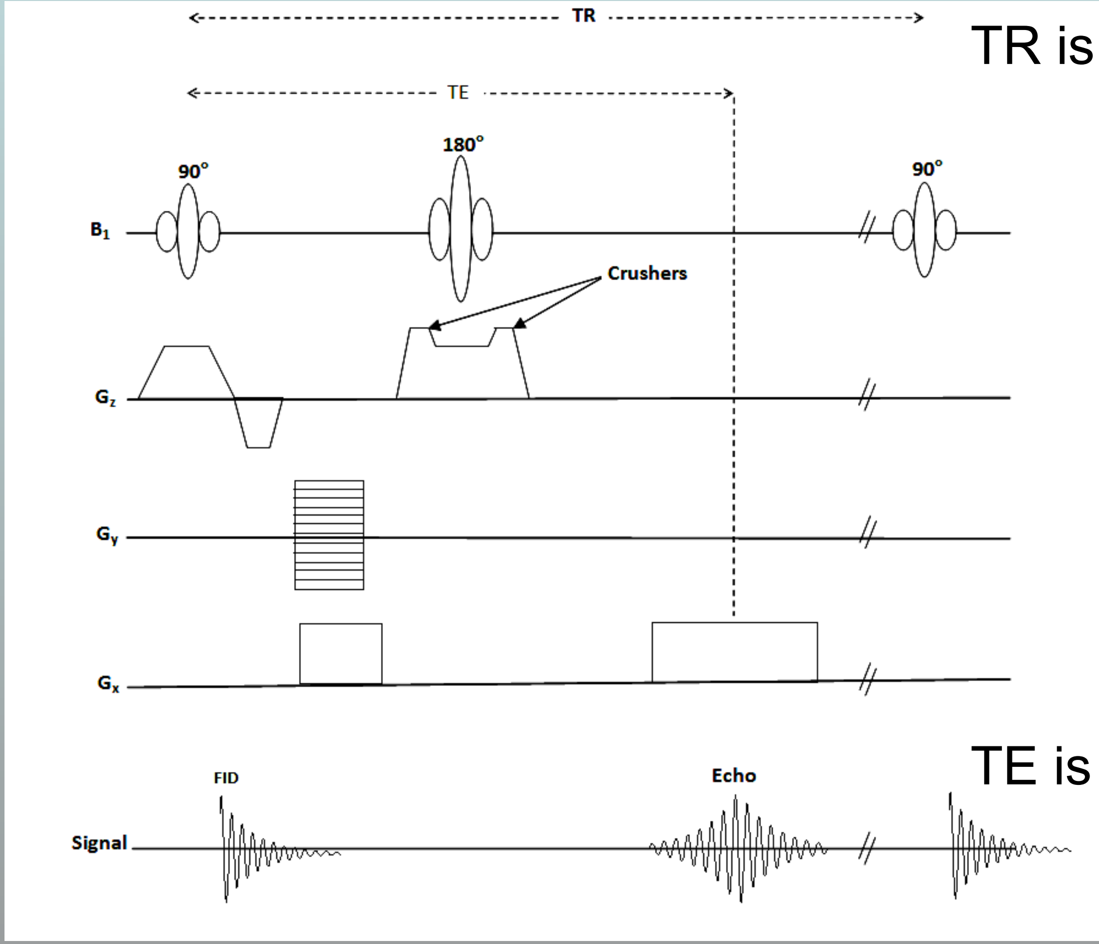

TR is repetition time

TE is the echo time

The pulse program establishes the slice, the field of view and the image resolution, but in the Fourier domain.

Bloch Equation / Relaxation

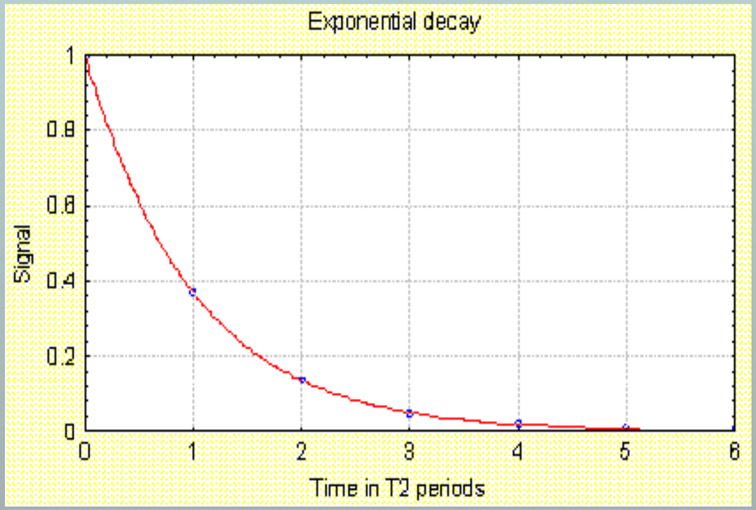

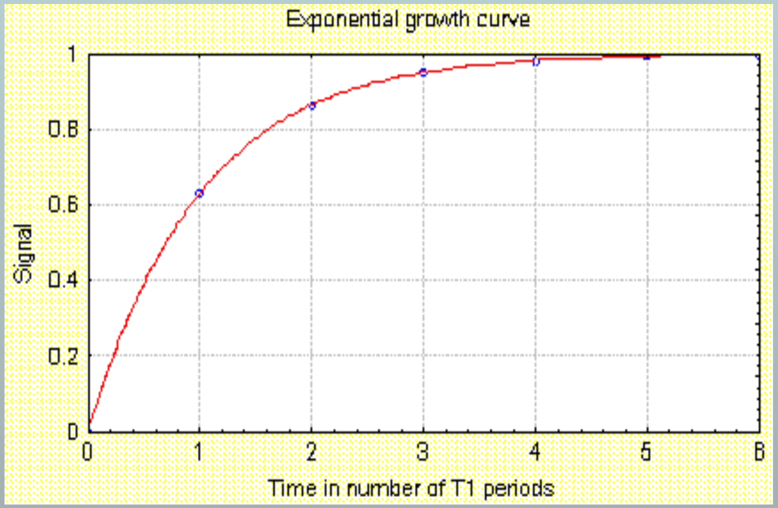

Each voxel in a tissue has its own characteristic T1 and T2.

These T1 and T2 values determine the fundamental image contrast

MRI of the Brain – Sagittal Slice

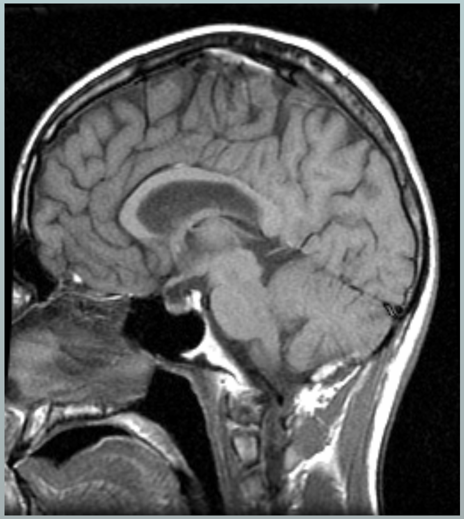

T1 Contrast
$T_E = 14$ ms
$T_R = 400$ ms

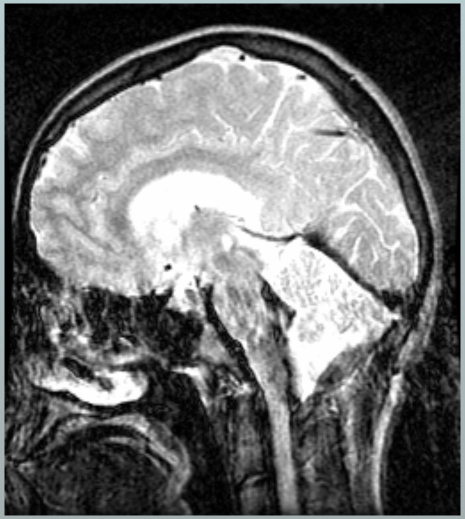

T2 Contrast
$T_E = 100$ ms
$T_R = 1500$ ms

Proton Density
$T_E = 14$ ms
$T_R = 1500$ ms

Brain Tumor- Axial Slice

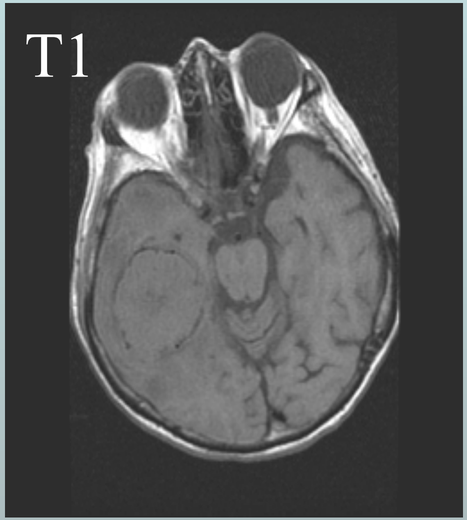

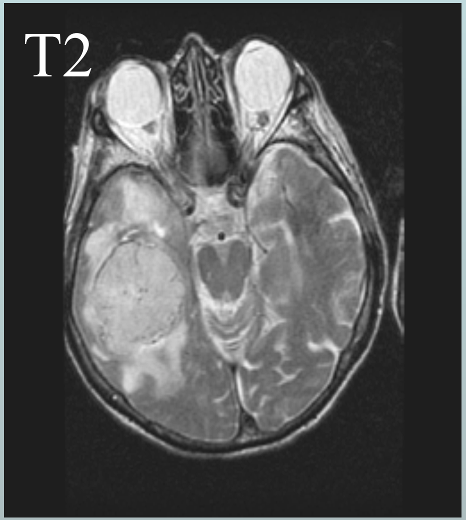

Post-Gd T_1

How can we use the diffusion of water to provide such image contrast?

Diffusion in NMR

Nuclear magnetic resonance (NMR) is an ideal method for investigating the self-diffusion of water because it is possible to "label" the molecules by manipulating the magnetization of the hydrogen nuclei without interfering with the process of diffusion.

This process can be "measured" using the Stejskal-Tanner gradient pulse pair:

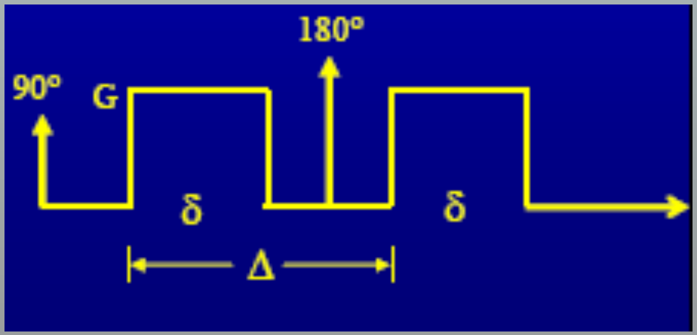

We will see "how" soon.

Diffusion in Medicine

NMR is hence a useful tool with which to measure the diffusion coefficient, D, in liquids, porous materials, and tissues. And MRI, when diffusion-weighted, is now used to detect and diagnosis pathology:

- **i) Tumors, (cystic, edema, solid; D increases with tumor stage)**
- **ii) Stroke, (in grey matter, D decreases immediately after onset)**
- **iii) White Matter Disease (D is less anisotropic)**

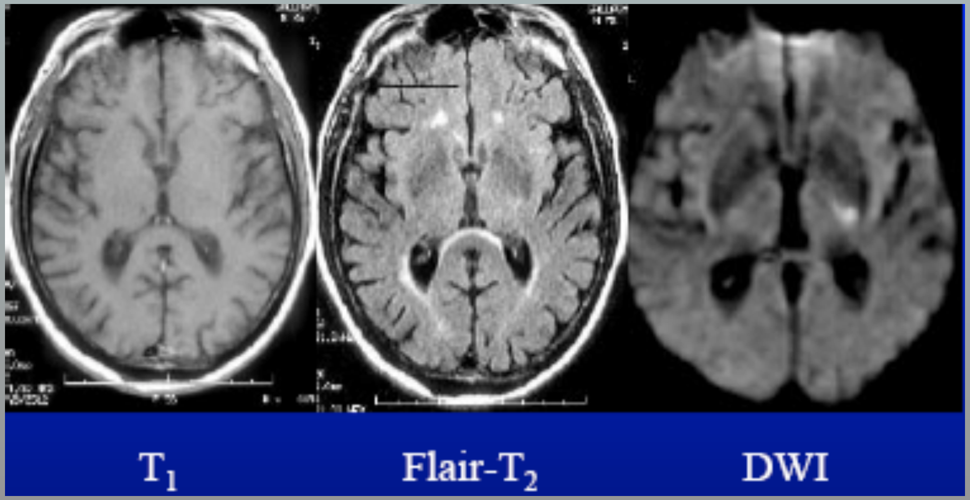

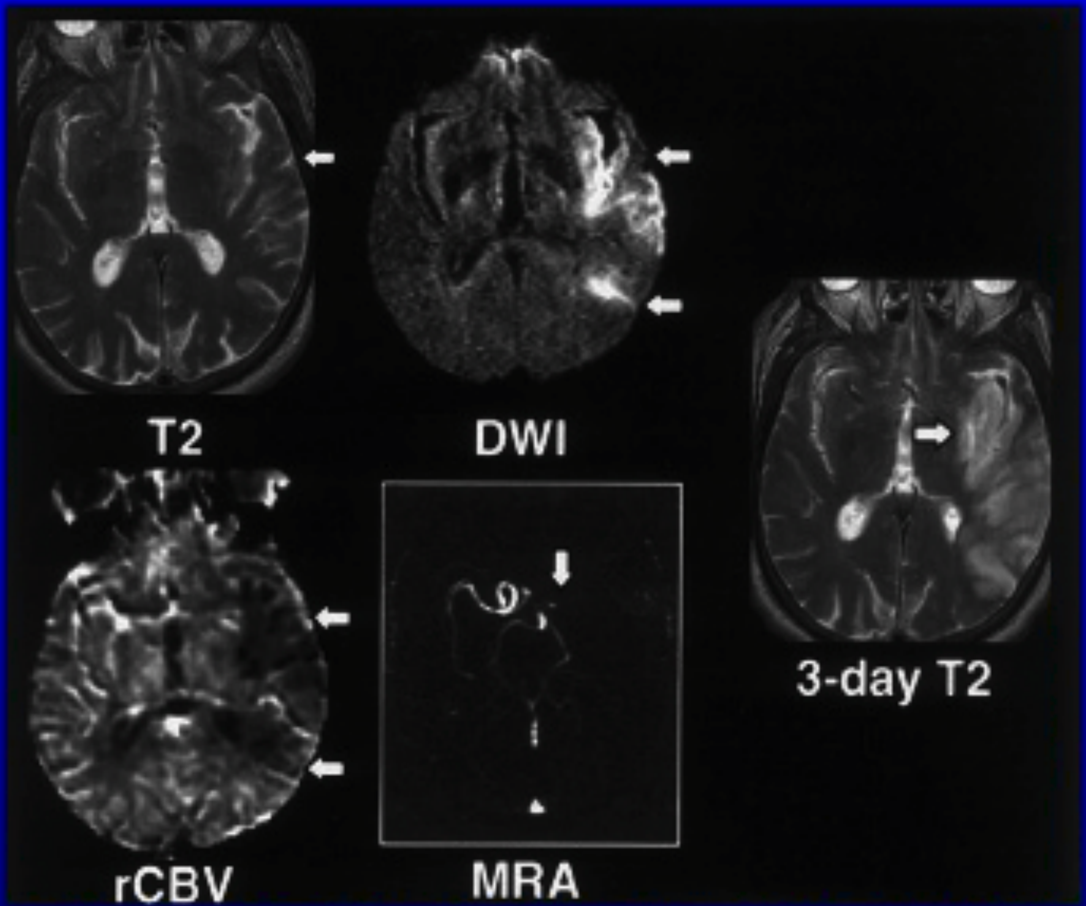

Progressive cortical infarction. A 62-year-old man had sudden onset of dense right hemiplegia 7 hours before his MRI study. The T2 sequence shows only a subtle increase in signal in a gyral pattern, whereas the DWI map shows an ischemic injury (arrow) mostly located in the insular and peri-insular cortex. The CBV map demonstrates a perfusion abnormality (arrow) much larger than the DWI abnormality. MRA demonstrates a left MCA stem occlusion (arrow). In the follow-up MRI the stroke has expanded beyond the initial area of perfusion abnormality (arrow).

Sorensen

Le Bihan, *Diffusion and Perfusion Magnetic Resonance Imaging*, 2004.

How can we use MRI to measure diffusion?

Neglecting precession, T_1 and T_2 relaxation, we can write the Bloch-Torrey PDE for Magnetization, **M**(**r**,t), as:

$$\frac{\partial \vec{M}(\vec{r},t)}{\partial t} = \gamma \vec{M}(\vec{r},t) \times \vec{B} + D\nabla^2 \vec{M}(\vec{r},t) \qquad \vec{B} = (\vec{r} \cdot \vec{G}(t))\hat{z}$$

where γ = 42.58 MHz/Tesla and D is the diffusion constant (mm^2/sec).

$$M_{xy}(\vec{r},t) = M_x(\vec{r},t) + iM_y(\vec{r},t) = M_0 A(t) \exp\left(-i\gamma \vec{r} \cdot \int_0^t G(t')\,dt'\right)$$

$$\frac{d \ln A(t)}{dt} = e^{i\gamma \vec{r} \cdot \int_0^t G(t')\,dt'} D\nabla^2 e^{-i\gamma \vec{r} \cdot \int_0^t G(t')\,dt'}$$

Bloch-Torrey PDE for Magnetization, **M**(**r**,t)

$$\ln A(t) = -D\gamma^2 \int_0^t \left[\left(\int_0^{t'} \vec{G}(t'')\,dt'' \right) \cdot \left(\int_0^{t'} \vec{G}(t'')\,dt'' \right) \right]$$

If $\vec{G}(t) = g(t)\hat{z}$ then for a pair of rectangular gradient pulses of amplitude g_0, duration δ, and separated by Δ.

$$M_{xy}(\vec{r}, g_0, \Delta, \delta) = M_0 \exp[-(\gamma g_0 \delta)^2 (\Delta - \delta/3) D]$$

Since the detected NMR signal is proportional to M_{xy} we have the simple result:

$$S = S_0 \exp(-bD)$$

$$b = (\gamma g_0 \delta)^2 (\Delta - \delta/3)$$

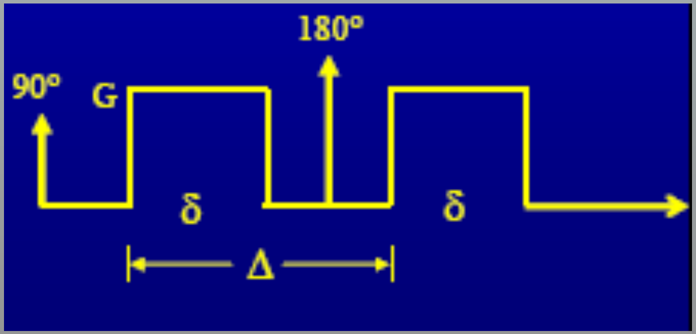

Map of D (x 10^{-3} mm^2/s)

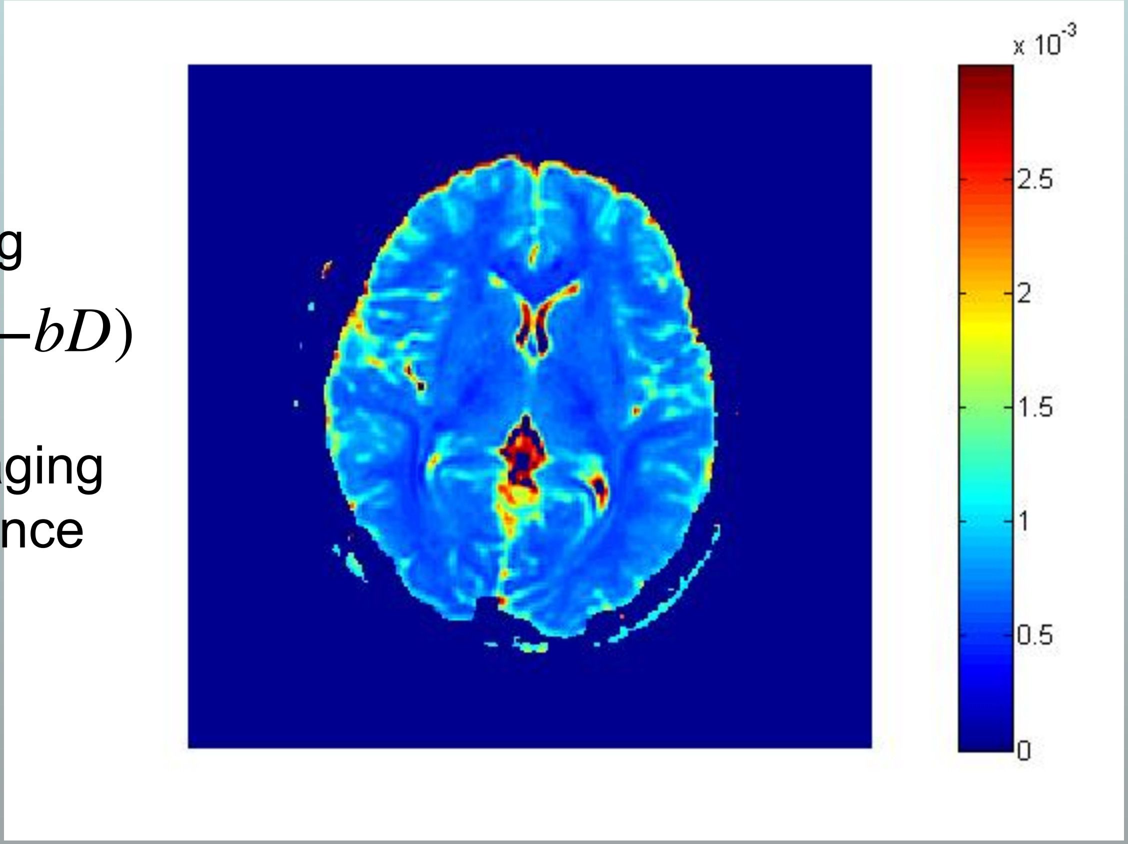

Using

$$S = S_0 \exp(-bD)$$

in an MR imaging pulse sequence

The diffusion map distinguishes white matter from gray matter, with the cerebral spinal fluid (CSF) giving the highest values.

How well does $S=S_0\exp[-(bD)]$ really work?

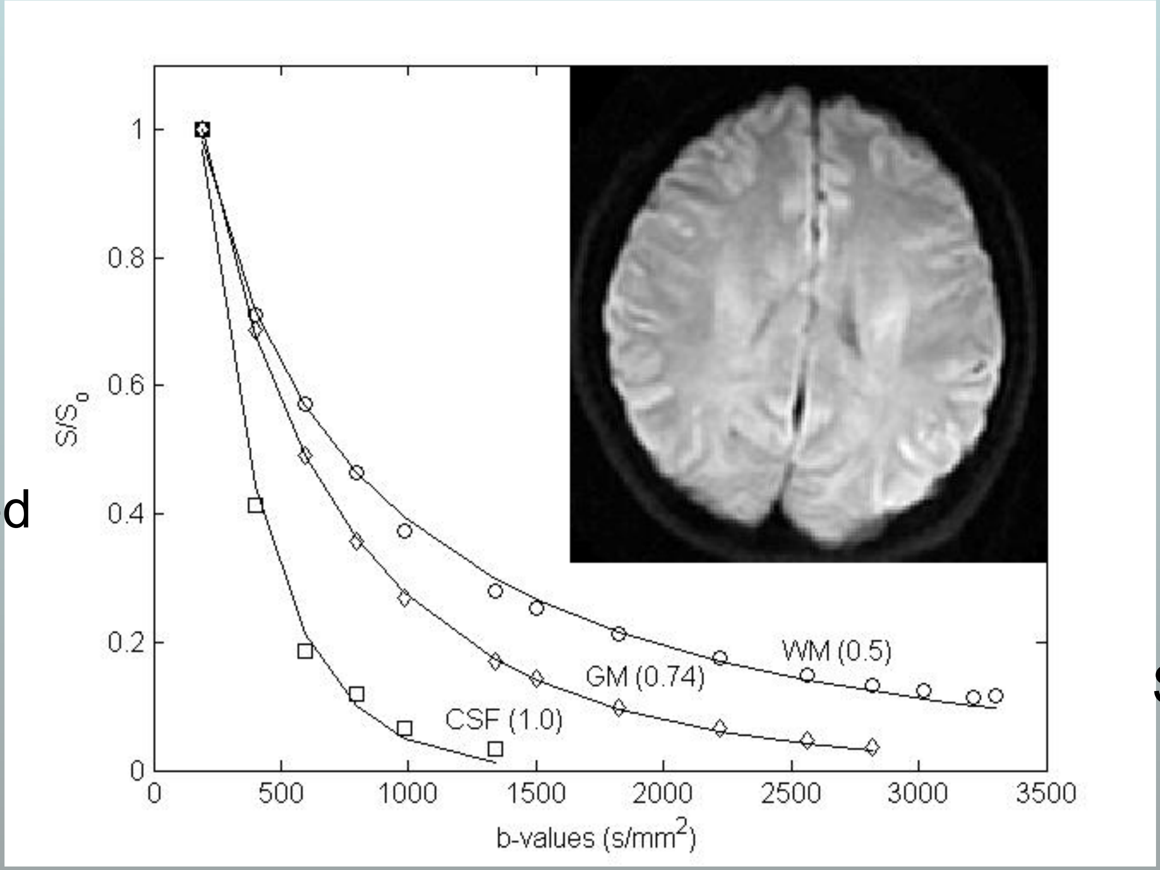

Try a stretched Exponential!

Heuristic!

$S=S_0\exp(-[bD]^\beta)$, with $0 < \beta < 1$

DW-EPI at 3T: TR/TE = 4000/97 ms, slice thickness = 3 mm, matrix 256 x 256 and FOV = 22 x 22 cm^2. Max b-value = 3,300 s/mm^2

The stretched exponential parameter β ($0 < \beta < 1$) also can provide a “map” of brain tissue.

$S=S_0\exp(-[bD]^{\beta})$,

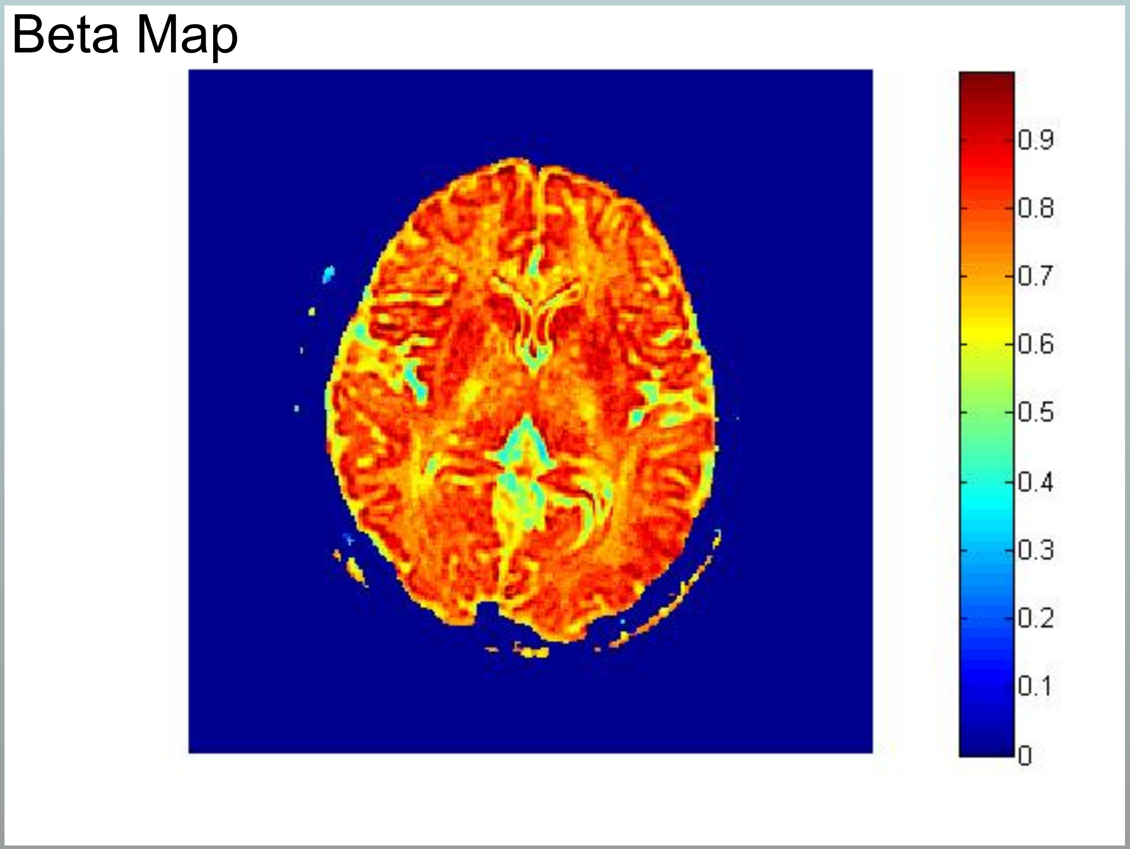

But why does it work and what does it mean? To answer this we will use fractional calculus.

Fractional Order Operators in Space (Riesz fractional derivative)

If we consider a well behaved function y(x) on (-∞, ∞) then we can define its Fourier transformation $y(\xi_x)$ through the integrals:

$$F\{y(x)\} = \hat{y}(\xi_x) = \int_{-\infty}^{\infty} y(x') e^{i\xi_x x'}\, dx'$$

Fourier

$$y(x) = F^{-1}\{\hat{y}(\xi_x)\} = \frac{1}{2\pi}\int_{-\infty}^{\infty} \hat{y}(\xi_x) e^{-\xi_x x}\, d\xi_x$$

Fractional Order Operators in Space (Riesz fractional derivative)

In the Fourier domain for 1 < β <2 we will define the Fourier transform of the fractional order derivative as:

$$\frac{d^\beta}{dx^\beta} g(x) \xrightarrow{F} (-i\xi_x)^\beta \hat{g}(\xi_x), \quad \frac{d^\beta}{d(-x)^\beta} g(x) \xrightarrow{F} (i\xi_x)^\beta \hat{g}(\xi_x)$$

Hence we can write,

$$\frac{d^\beta}{d\left|x\right|^\beta} g(x) = -\frac{1}{2\cos(\beta\pi/2)}\left[\frac{d^\beta}{dx^\beta} + \frac{d^\beta}{d(-x)^\beta}\right] g(x)$$

$$\frac{d^\beta}{d\left|x\right|^\beta} g(x) \xrightarrow{F} -\left|\xi_x\right|^\beta \hat{g}(\xi_x)$$

In the case of $y(x) = e^{iax}$, we have

$$D_x^\beta (e^{iax}) = -\left|a\right|^\beta e^{iax}$$

Riesz

Riesz fractional derivative

$$D_x^{\beta}(e^{-ax^2}) = \frac{a^{\beta/2}}{\pi}\sin\left(\frac{\pi\beta}{2}\right)\Gamma\left(\frac{-\beta}{2}\right)\Gamma(1+\beta)\,{}_1F_1\left(\frac{1+\beta}{2};\frac{1}{2};-ax^2\right)$$

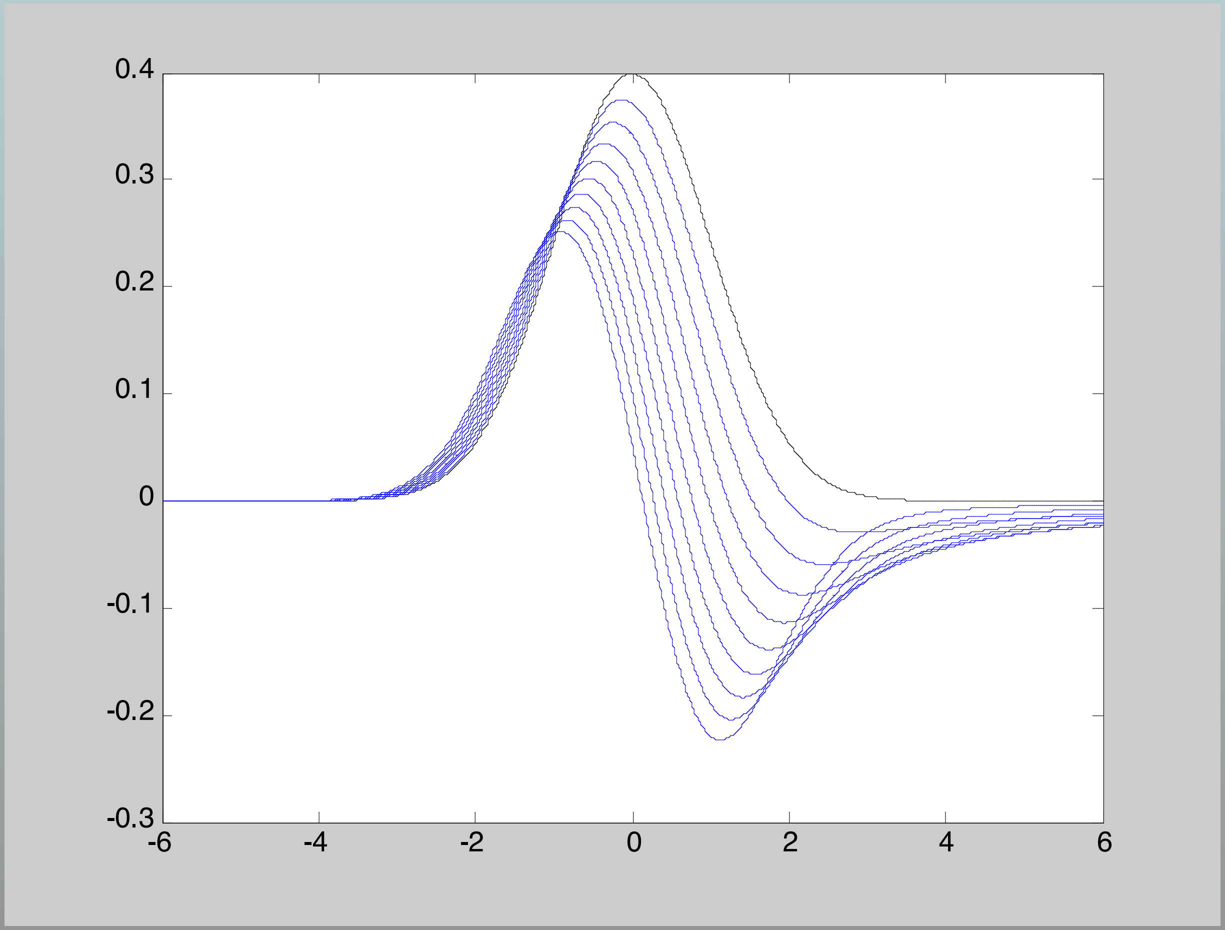

Fractional Order Operators in Time (Caputo fractional derivative)

If we consider a well behaved function *y(t)* on [0,∞) then we can define its Laplace transformation through the integrals:

$$L\{y(t)\} = \hat{y}(s) = \int_0^\infty y(t')e^{-st'}dt'$$

$$y(t) = L^{-1}\{\hat{y}(s)\} = \frac{1}{2\pi i}\int_{c-i\infty}^{c+i\infty} y(s)e^{st}\,ds$$

Riemann

In the Laplace domain for (0 < α < 1), we will define the Caputo fractional order form of the Riemann-Liouville derivative as

$$L\{{}_o^C D_t^\alpha y(t)\} = s^\alpha y(s) - s^{\alpha-1} y(0^+)$$

Liouville

Fractional Order Operators in Time (Laplace Domain)

Hence we can write

$$ {}_{o}^{C}D_t^{\alpha} y(t) = L^{-1}\left\{ s^{\alpha} L\{y(t)\} \right\} - \frac{y(0^+)t^{-\alpha}}{\Gamma(1-\alpha)} $$

where $\Gamma(1-\alpha) = \int_0^{\infty} e^{-u}u^{-\alpha}\,du$ is the Gamma function.

In the time domain for ($0 < \alpha < 1$)

$$ {}_{o}^{C}D_t^{\alpha} u(t) = 0, \textit{where } u(t) \textit{ is the unit step function} $$

$$ {}_{o}^{C}D_t^{\alpha}\left[t^k u(t) \right] = \frac{\Gamma(k+1)t^{k-\alpha}}{\Gamma(k-\alpha+1)}, \textit{ for } k \geq 0 $$

$$ {}_{o}^{C}D_t^{\alpha}\left[E_{\alpha}(\lambda t^{\alpha}) \right] = \lambda E_{\alpha}(\lambda t^{\alpha}), \textit{ here } E_{\alpha}(z) \textit{ is the Mittag-Leffler function} $$

Laplace

Fractional Order Bloch-Torrey PDE for Magnetization, **M**(**r**,t)

Magin et al, JMR 190, 255, 2008

$$\boldsymbol{\tau}^{\alpha-1}\,{}_0^C D_t^{\alpha}[M_{xy}(\vec{r},t)] = -i\gamma(\vec{r}\cdot\vec{G}(t))M_{xy}(\vec{r},t) + D\mu^{\beta-2}\;{}_R D_{|\vec{r}|}^{\beta}[M_{xy}(\vec{r},t)]$$

Here $\boldsymbol{\tau}^{\alpha-1}\,{}_0^C D_t^{\alpha}$ is the Caputo fractional time derivative, $0 < \alpha < 1$,

and $\mu^{\beta-2}\;{}_R D_{|\vec{r}|}^{\beta}$ is the Riesz fractional space derivative, $1 < \beta < 2$.

For a Stejskal -Tanner gradient pair pulse sequence, and for $\alpha = 1$, we can write:

$$S = S_0 \exp\left[-(\gamma g_0 \delta)^{\beta} D\mu^{\beta-2}\left(\Delta - \frac{(\beta-1)}{(\beta+1)}\delta\right)\right]$$

Here D is the apparent diffusion coefficient, mm^2/sec.

PGSE (Stejskal-Tanner)

Changing β (0.3 – 1.0) and μ (5−55 μm)

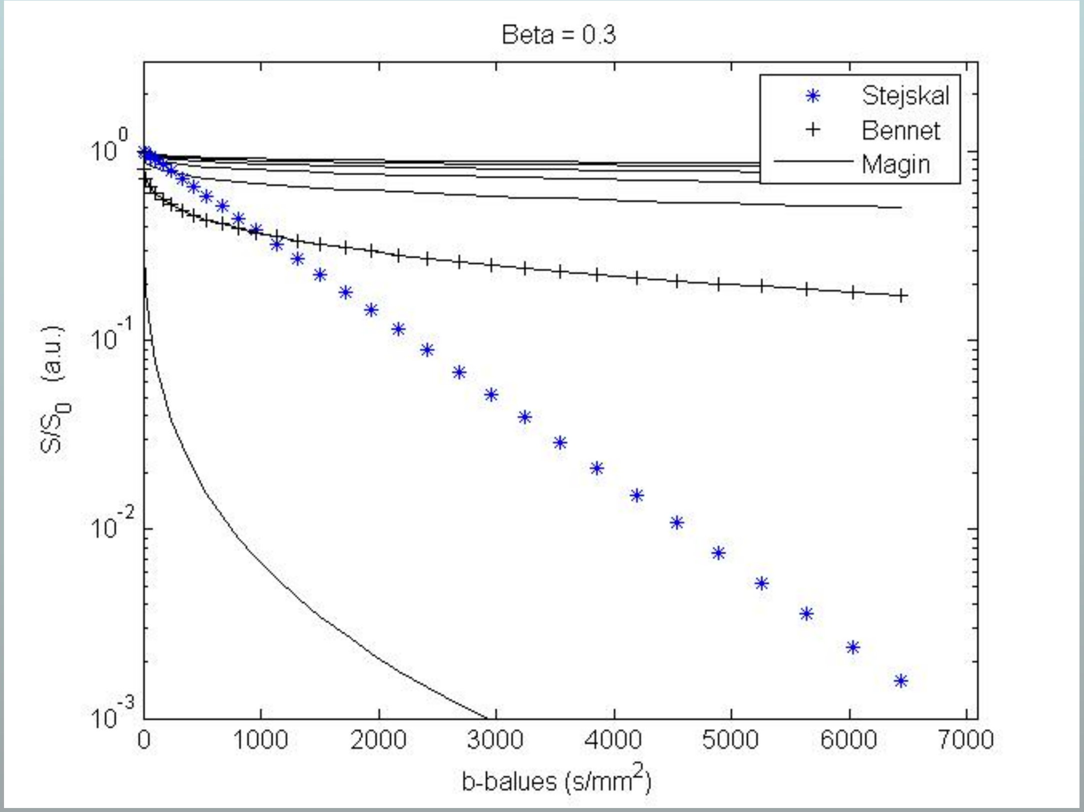

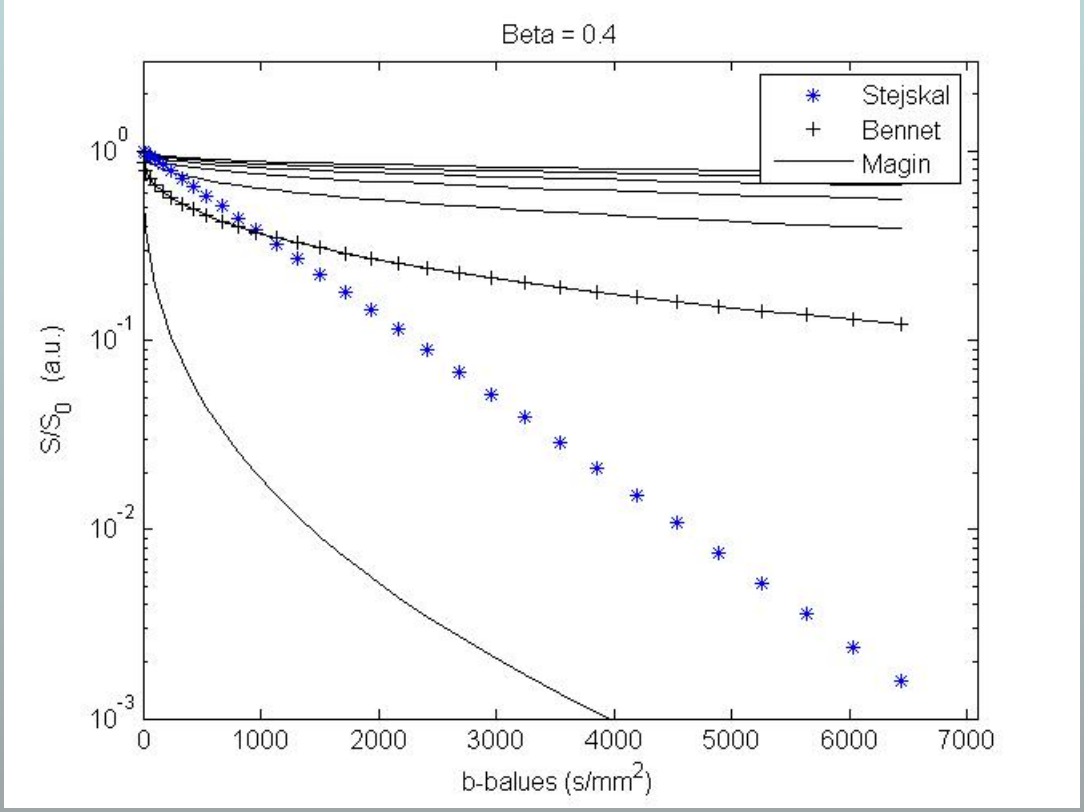
Beta = 0.4
Stejskal
Bennet
Magin
S/S0 (a.u.)
b-balues (s/mm2)
10^0
10^-1
10^-2
10^-3
0
1000
2000
3000
4000
5000
6000
7000

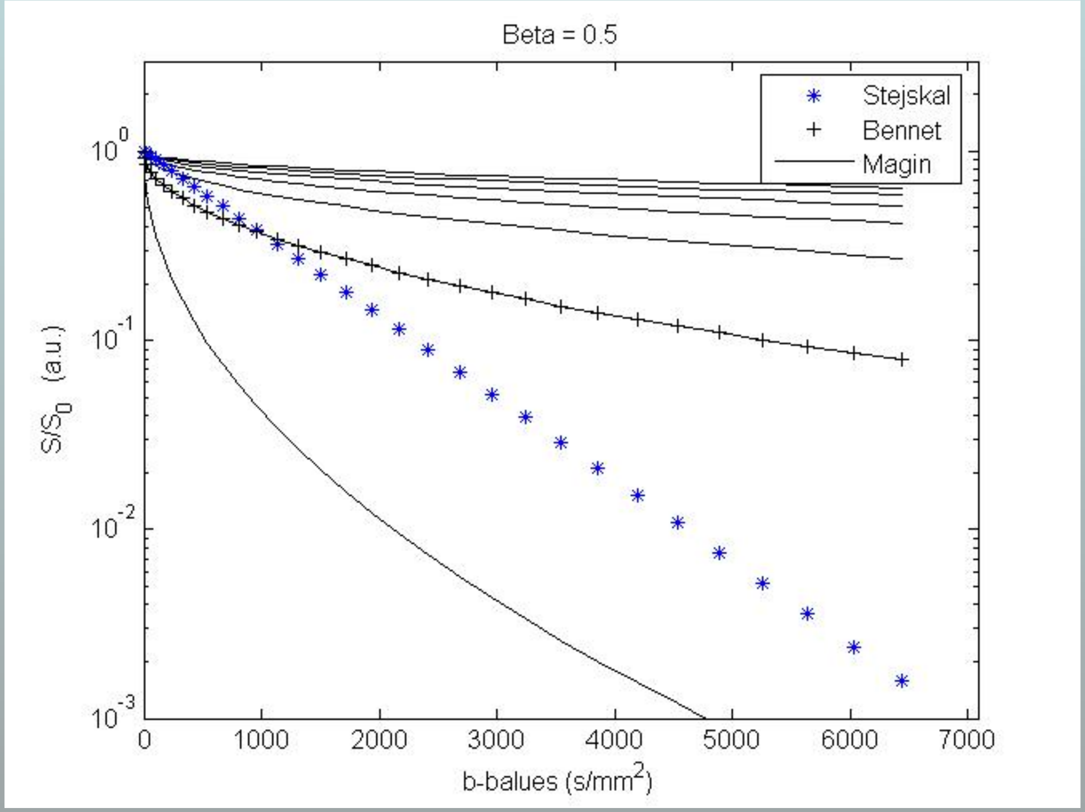
Beta = 0.5
Stejskal
Bennet
Magin
S/S0 (a.u.)
b-balues (s/mm2)
10^0
10^-1
10^-2
10^-3
0
1000
2000
3000
4000
5000
6000
7000

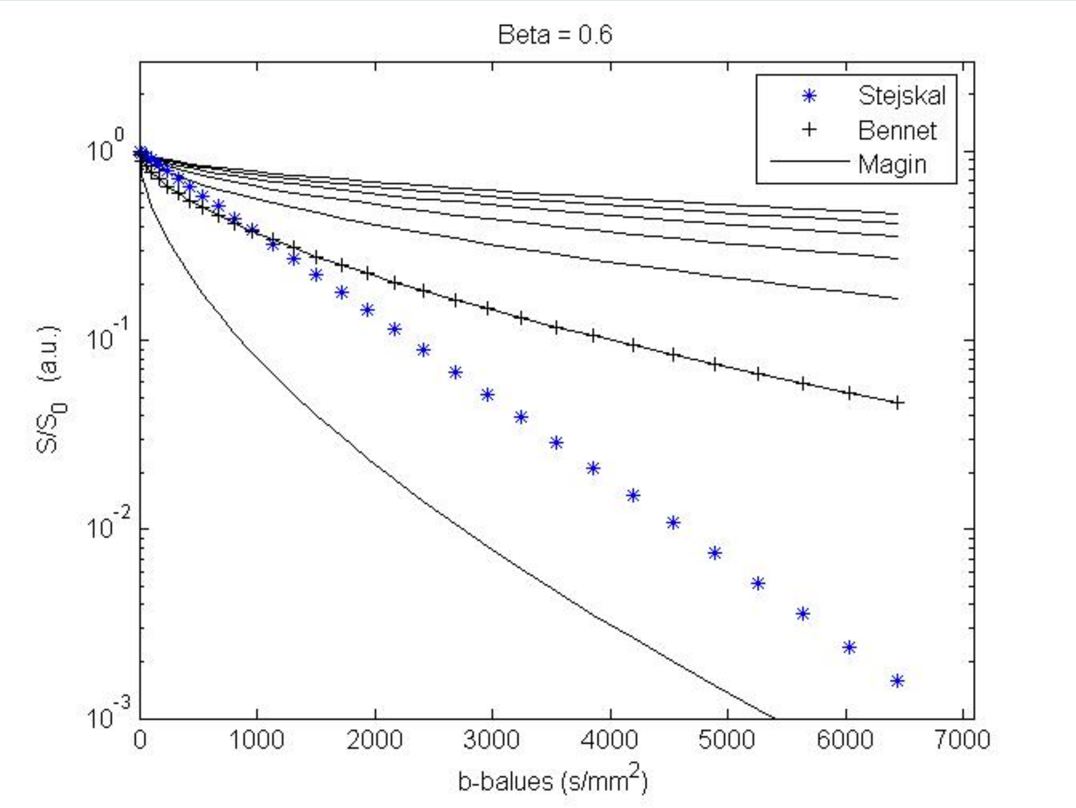
Beta = 0.6
Stejskal
Bennet
Magin
10^0
10^{-1}
10^{-2}
10^{-3}
S/S_0 (a.u.)
0
1000
2000
3000
4000
5000
6000
7000
b-balues (s/mm^2)

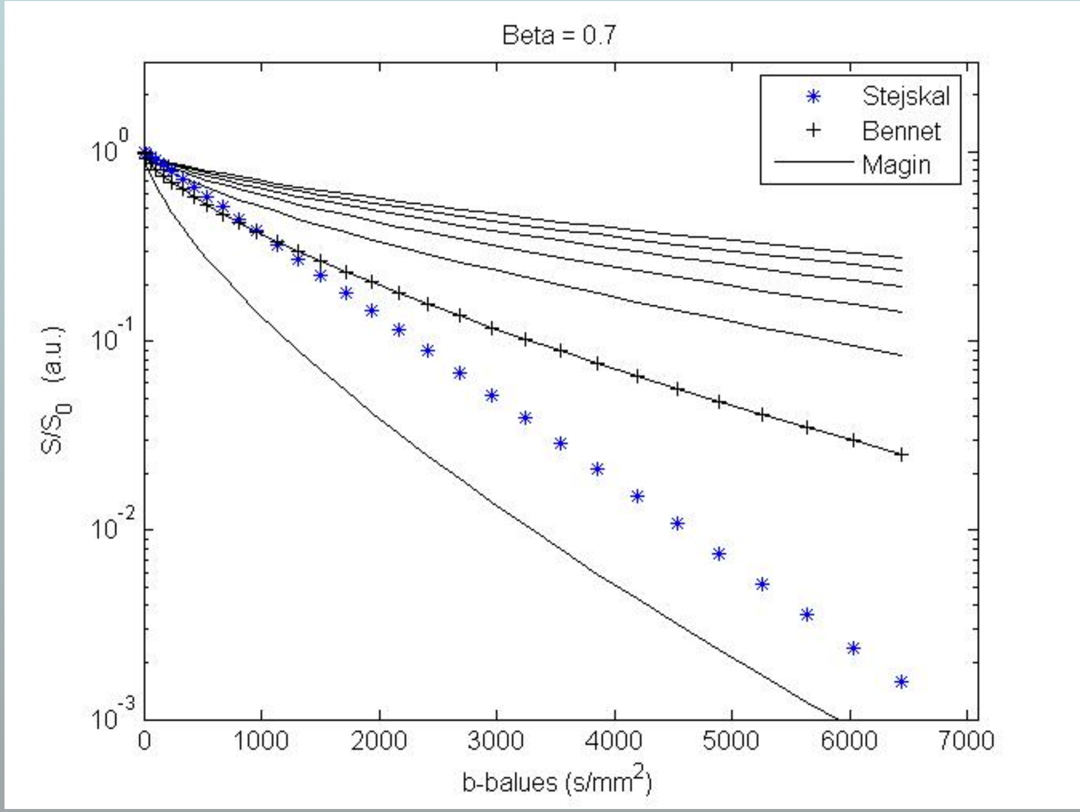
Beta = 0.7
Stejskal
Bennet
Magin
S/S0 (a.u.)
10^0
10^-1
10^-2
10^-3
0
1000
2000
3000
4000
5000
6000
7000
b-balues (s/mm2)

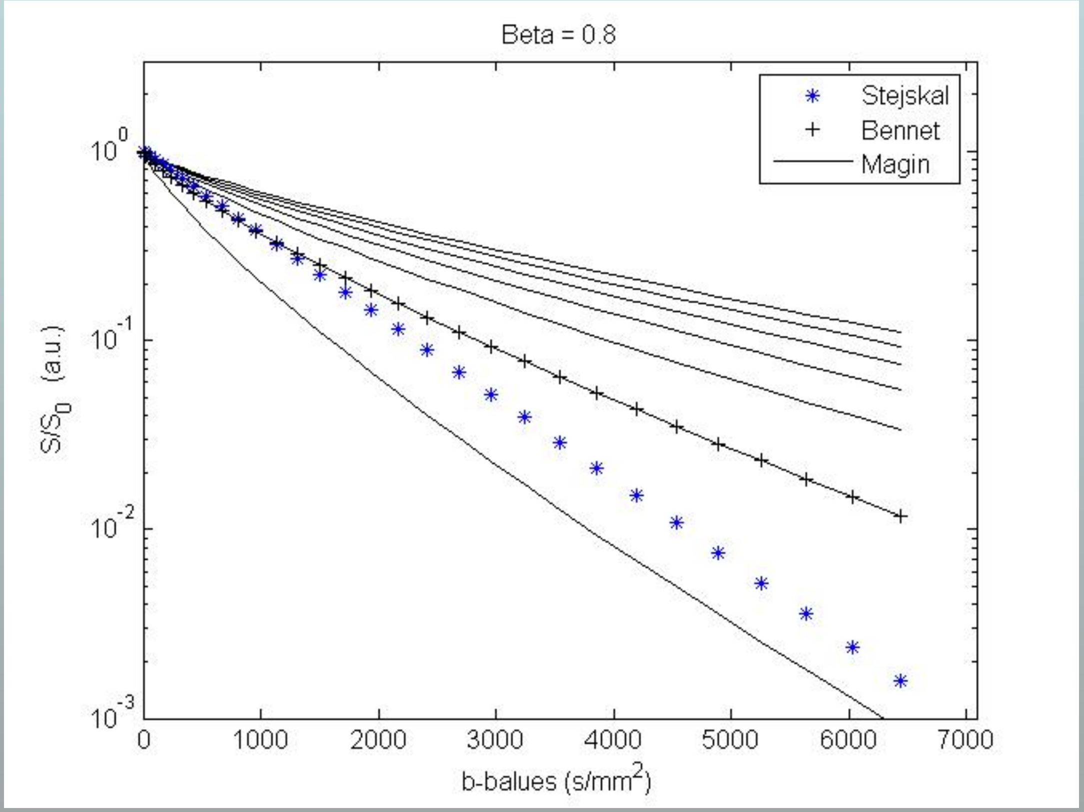
Beta = 0.8
Stejskal
Bennet
Magin
10^0
10^{-1}
10^{-2}
10^{-3}
S/S$_0$ (a.u.)
0
1000
2000
3000
4000
5000
6000
7000
b-balues (s/mm^2)

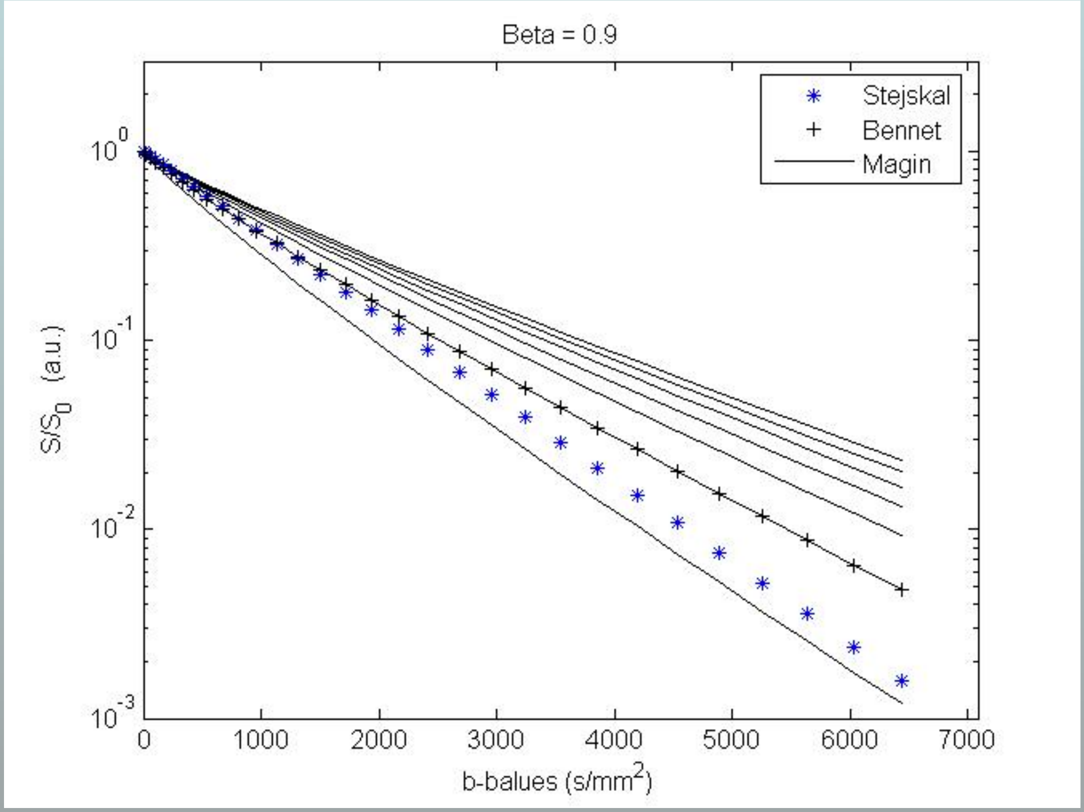
Beta = 0.9
Stejskal
Bennet
Magin
S/S0 (a.u.)
10^0
10^-1
10^-2
10^-3
0
1000
2000
3000
4000
5000
6000
7000
b-balues (s/mm2)

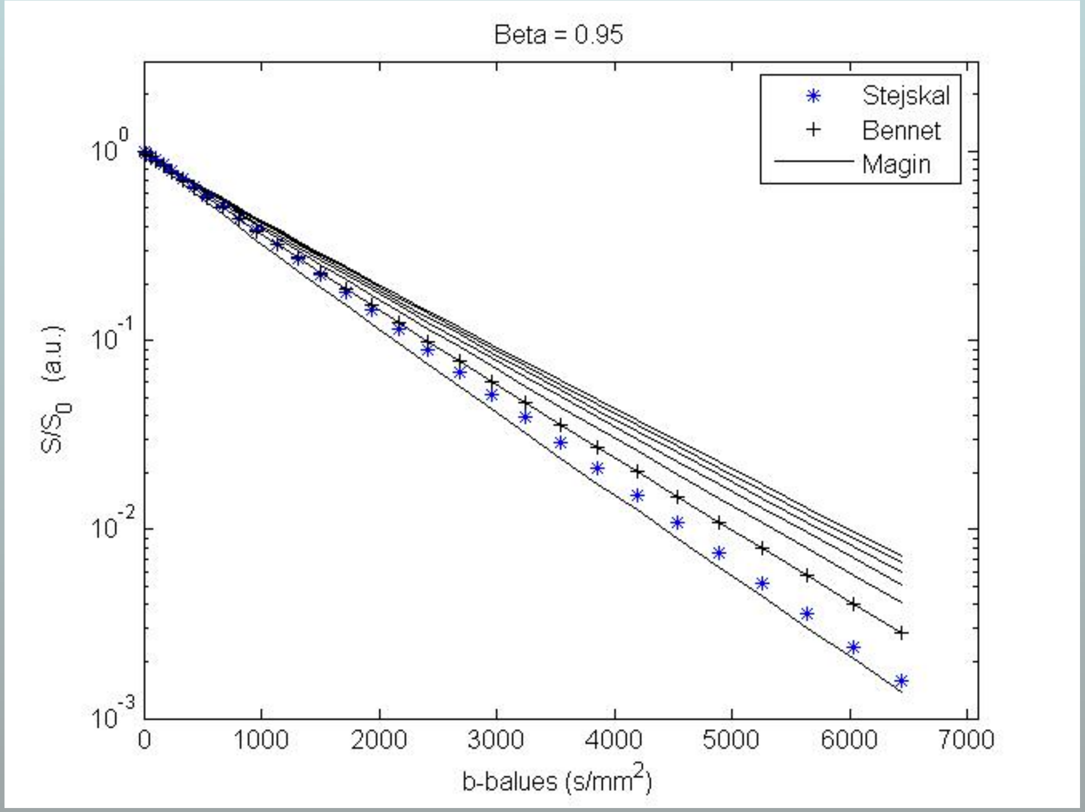
Beta = 0.95
Stejskal
Bennet
Magin
10^0
10^{-1}
10^{-2}
10^{-3}
S/S_0 (a.u.)
0
1000
2000
3000
4000
5000
6000
7000
b-balues (s/mm^2)

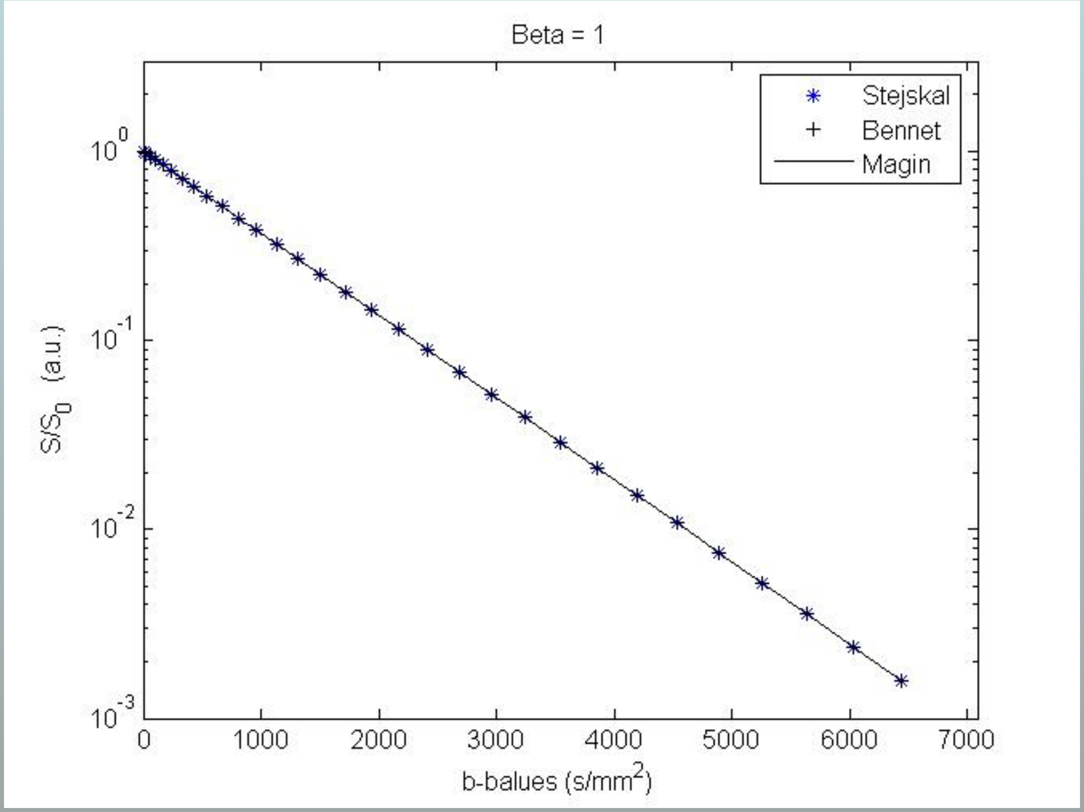
Beta = 1
Stejskal
Bennet
Magin
10^{0}
10^{-1}
10^{-2}
10^{-3}
S/S$_0$ (a.u.)
0
1000
2000
3000
4000
5000
6000
7000
b-balues (s/mm^2)

Fractional Order Bloch-Torrey PDE for Magnetization, **M**(**r**,t) – General Case:

Hanyga and Seredyńska, JMR 220, 85, 2012

$$S = S_0 (M_{\alpha,\beta})^2 E_\alpha[-(\gamma g_0 \delta)^\beta D_{\alpha,\beta} (\Delta - \delta)^\alpha]$$

$$M_{\alpha,\beta} = F_{\alpha,\beta}[(\gamma g_0 \delta)^\beta D_{\alpha,\beta} \delta^\alpha]$$

Note, that $E_\alpha(z^\alpha)$ is the single parameter Mittag-Leffler function, but that

$$F_{\alpha,\beta}(z) = E_{\alpha,1+\beta/\alpha,\beta/\alpha}(z)$$

is the Kilbas-Saigo function, Kilbas et al, 2007

Let's consider some particular cases.

Fractional Order Bloch-Torrey PDE for Magnetization, **M**(**r**,t)

$M_{\alpha,\beta}$	$1<\beta<2$	$\beta=2$
$0<\alpha<1$	$F_{\alpha,\beta}[(\gamma g_0\delta)^{\beta}D_{\alpha,\beta}\delta^{\alpha}]$	$F_{\alpha,2}[(\gamma g_0\delta)^{2}D_{\alpha,2}\delta^{\alpha}]$
$\alpha=1$	$F_{1,\beta}[(\gamma g_0\delta)^{\beta}D_{1,\beta}\delta]=$ $\exp[-(\gamma g_0\delta)^{\beta}D_{1,\beta}\delta/(\beta+1)]$	$F_{1,2}[(\gamma g_0\delta)^{2}D_{1,2}\delta]=$ $\exp[-(\gamma g_0\delta)^{2}D_{1,2}\delta/3]$

Here the time and space constants are incorporated into $D_{\alpha,\beta}$.

Fractional Order Bloch-Torrey PDE for Magnetization, **M**(**r**,t)

S/S_0	$1<\beta<2$	$\beta=2$
$0<\alpha<1$	$(M_{\alpha,\beta})^2 E_\alpha[-(\gamma g_0\delta)^\beta D_{\alpha,\beta}(\Delta-\delta)^\alpha]$	$(M_{\alpha,2})^2 E_\alpha[-(\gamma g_0\delta)^2 D_{\alpha,2}(\Delta-\delta)^\alpha]$
$\alpha=1$	$(M_{1,\beta})^2 E_1[-(\gamma g_0\delta)^\beta D_{1,\beta}(\Delta-\delta)]=$ $\exp[-(\gamma g_0\delta)^\beta D_{1,\beta}(\Delta-\frac{(\beta-1)}{(\beta+1)}\delta)]$	$(M_{1,2})^2 F_{1,2}[-(\gamma g_0\delta)^2 D_{1,2}(\Delta-\delta)]=$ $\exp[-(\gamma g_0\delta)^2 D_{1,2}(\Delta-\frac{\delta}{3})]=\exp(-bD)$

Here the time and space constants are incorporated into $D_{\alpha,\beta}$.

Fractional Order Bloch-Torrey PDE for Magnetization, **M**(**r**,t) – Short Pulse Approx.

$$S = S_0 (M_{\alpha,\beta})^2 E_\alpha[-(\gamma g_0 \delta)^\beta D_{\alpha,\beta} (\Delta - \delta)^\alpha]$$

$$M_{\alpha,\beta} = F_{\alpha,\beta}[(\gamma g_0 \delta)^\beta D_{\alpha,\beta} \delta^\alpha]$$

In the short gradient pulse approximation, $\Delta >> \delta$, $g_0\delta$ constant, we obtain:

$$S = S_0 E_\alpha[-(\gamma g_0 \delta)^\beta D_{\alpha,\beta} (\Delta)^\alpha]$$

which for $k = \gamma g_0 \delta$ is the solution to the fractional order diffusion equation.

We can see this easily from…

The Diffusion Equation - Generalized

$$\frac{\partial P(x,t)}{\partial t} = D_{1,2}\frac{\partial^2 P(x,t)}{\partial |x|^2}$$

Where $D_{1,2}$ is the diffusion coefficient (e.g. mm^2/s).

The Diffusion Equation - Generalized

$$\frac{\partial P(x,t)}{\partial t} = D_{1,2} \frac{\partial^2 P(x,t)}{\partial |x|^2}$$

$$\frac{\partial^\alpha P(x,t)}{\partial t^\alpha} = D_{\alpha,\beta} \frac{\partial^\beta P(x,t)}{\partial |x|^\beta}$$

for $0 < \alpha \leq 1$ and $0 < \beta \leq 2$

Where $D_{1,2}$ is the diffusion coefficient (e.g. mm^2/s).

Where $D_{\alpha,\beta}$ is the diffusion coefficient (e.g. mm^β/s^α).

Application of the Laplace and Fourier transforms

$$p(k,s) = \frac{s^{\alpha-1}}{s^{\alpha} + D_{\alpha,\beta}|k|^{\beta}}$$

Taking the inverse Laplace transform

$$p(k,t) = E_{\alpha}\big(-D_{\alpha,\beta}|k|^{\beta}t^{\alpha}\big)$$

Here, $E_{\alpha}[-z^{\alpha}]$ is the single parameter Mittag-Leffler function.

Anomalous Diffusion (CTRW)

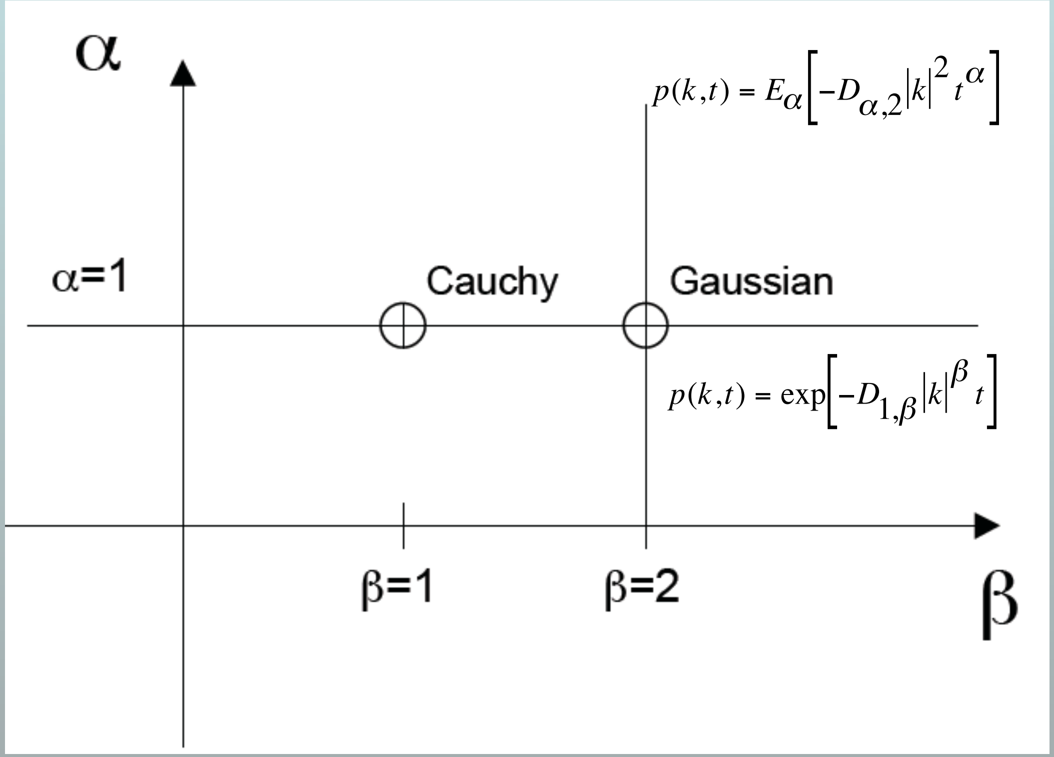

Anomalous diffusion phase diagram with respect to fractional order space parameter, β, and fractional order time parameter, α.

Metzler and Klafter, Phys Repts. 339; 1-77, 2003

Anomalous Diffusion Phase Diagram

$$\langle x^2(t) \rangle \sim t^{2\alpha/\beta}$$

Generalized Solution to the Diffusion Equation

$$p(k,t) = E_\alpha\big(- D_{\alpha,\beta}|k|^\beta t^\alpha \big)$$

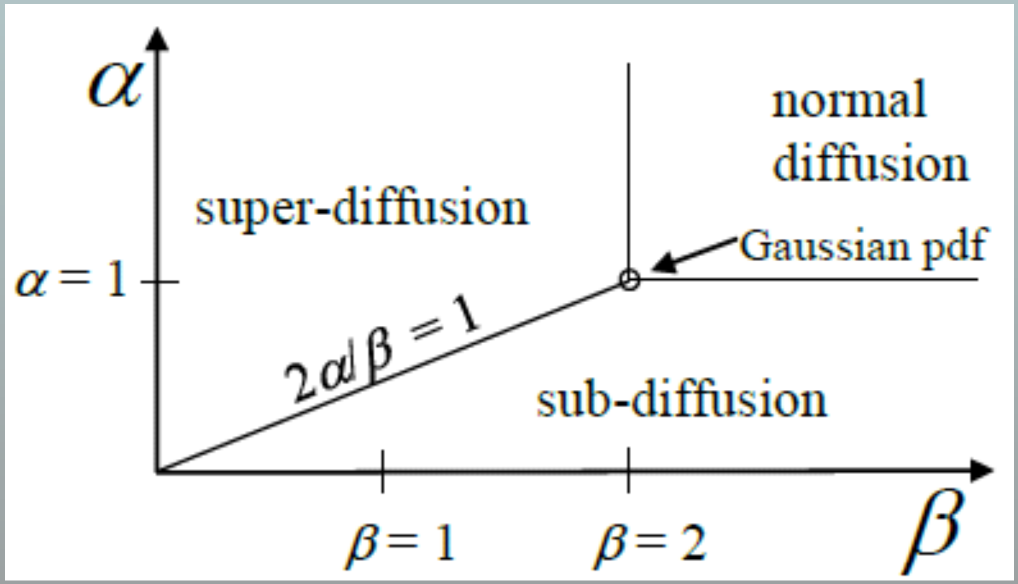

adapted from R. Metzler and J. Klafter. *Physics Reports*, 339(1):1-77, 2000.

Diffusion Simulations on Fractal Domains

(Özarslan et al., JMR, 183;315, 2006)

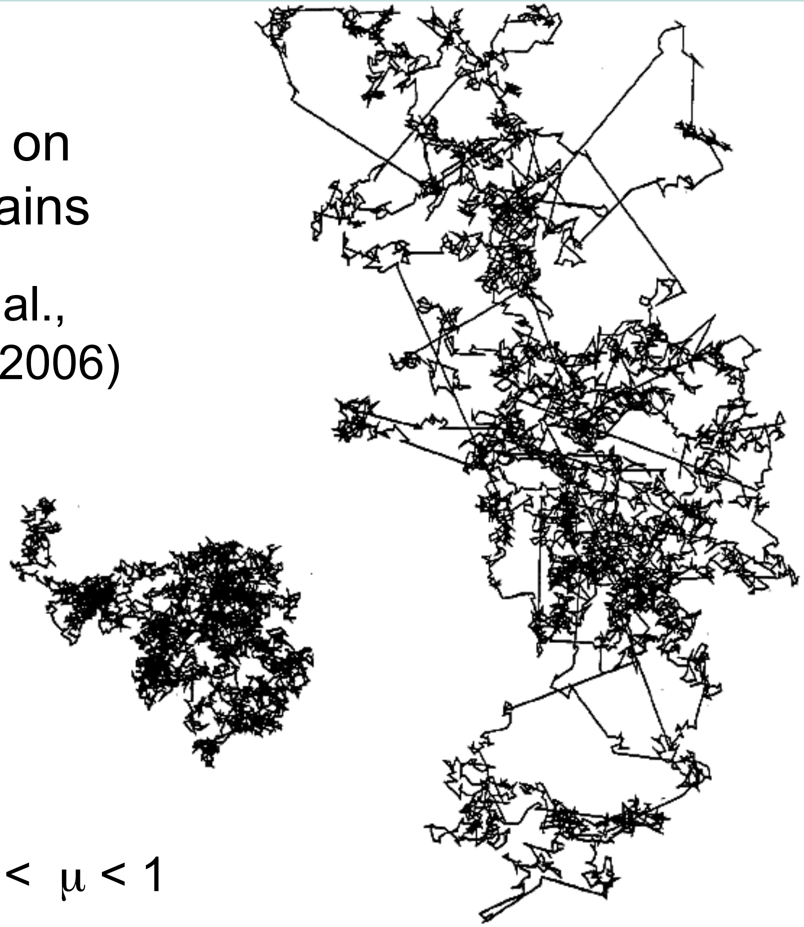

Subdiffusion, $0 < \mu < 1$

Superdiffusion

$\mu = 1.5$

Fig. 11. Comparison of the trajectories of a Brownian or subdiffusive random walk (left) and a Lévy walk with index $\mu = 1.5$ (right). Whereas both trajectories are statistically self-similar, the Lévy walk trajectory possesses a fractal dimension, characterising the island structure of clusters of smaller steps, connected by a long step. Both walks are drawn for the same number of steps (approx. 7000).

Model for Entropy MRI Experiments

$$p(k,t) = E_\alpha\left(-D_{\alpha,\beta}|k|^\beta t^\alpha\right)$$

↓ ↓

$$p(q,\bar{\Delta}) = E_\alpha\left(-D_{\alpha,\beta}\,|q|^\beta\,\bar{\Delta}^\alpha\right)$$

$$H(q,\Delta) = -\sum_{i=1}^{N} \frac{\hat{p}(q,\Delta)_i \ln[\hat{p}(q,\Delta)_i]}{ln(N)}$$

Here, $\hat{p}(q,\Delta)$ is the individual contribution to the normalized power spectrum and the ln(N) term is a normalization factor such that $0 < H(q,\Delta) < 1$.

Entropy Surface

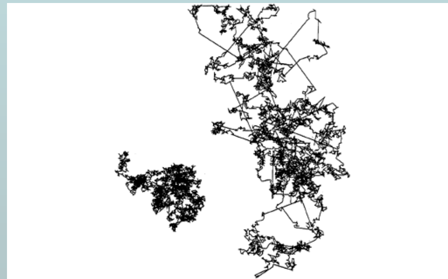

Fig. 11. Comparison of the trajectories of a Brownian or subdiffusive random walk (left) and a Lévy walk with index $\mu = 1.5$ (right). Whereas both trajectories are statistically self-similar, the Lévy walk trajectory possesses a fractal dimension, characterising the island structure of clusters of smaller steps, connected by a long step. Both walks are drawn for the same number of steps (approx. 7000).

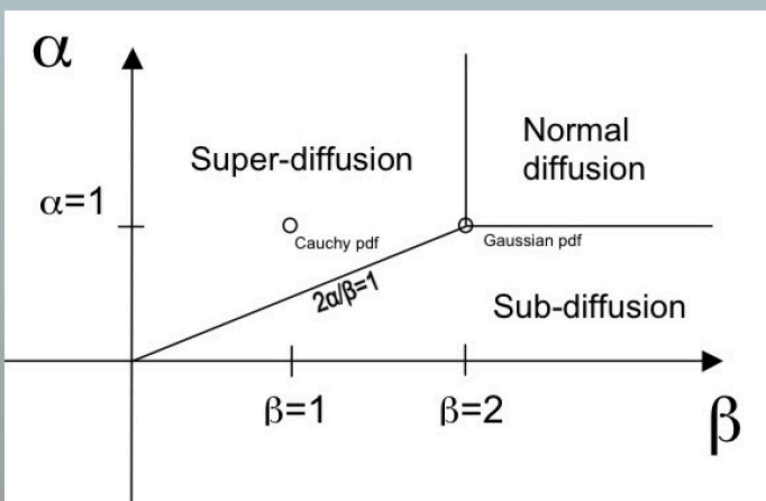

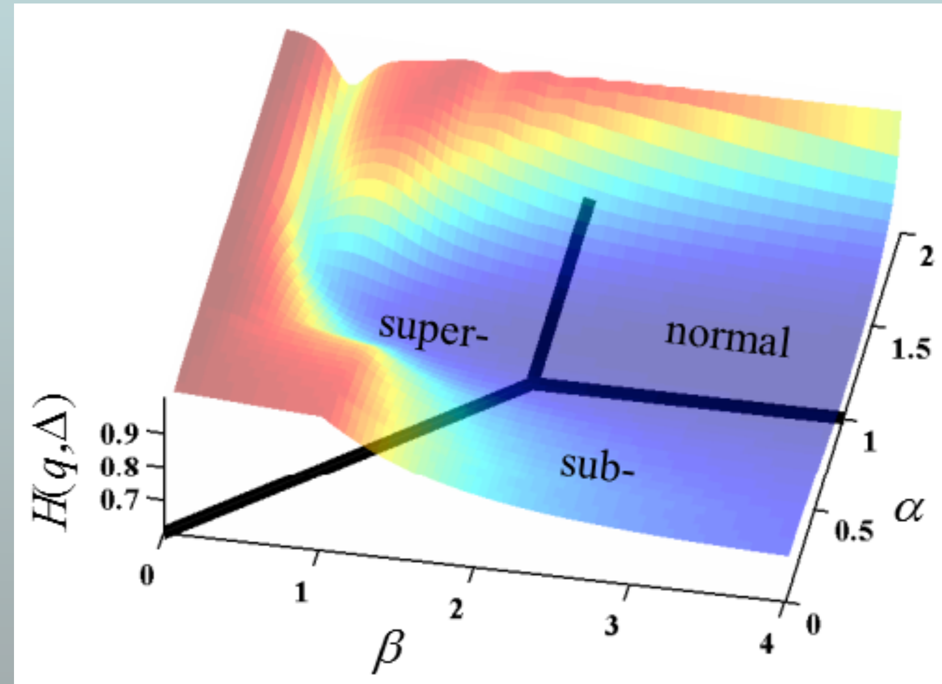

How can we apply this model to describe brain tissue?

Experimental Setup

- Fixed rat brain (4 % PFD) soaked overnight in phosphate buffered saline and imaged in Fluorinert
- Bruker 17.6 T, 750 MHz, 89 mm bore
- Pulsed Gradient Stimulated Echo (PGSTE) pulse sequence
  - TR=2 sec, TE=28 ms; with b-values up to 24,000 s/mm^2; NA = 2, 3 orthogonal gradient directions; 1 slice; thickness = 1 mm
- T1 correction via variable TR data collection
- δ=3.5 ms, Δ=20-400 ms, g=275-1,400 mT/m

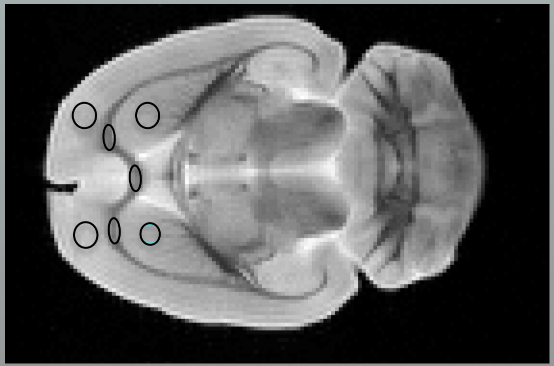

Model for Diffusion MRI Experiments

$$S/S_0 = exp(-bD) \quad b = q^2(\bar{\Delta}) \quad \bar{\Delta} = \Delta - \delta/3$$

Diffusion gradient strength (e.g. *mm*$^{-2}$)

Diffusion mixing time (e.g. *ms*)

Gradient pulse duration

Model for Diffusion MRI Experiments

$$S = S_0 exp(-bD) \qquad b = q^2(\bar{\Delta}) \qquad \bar{\Delta} = \Delta - \delta/3$$

$$p(k,t) = E_\alpha\big(- D_{\alpha,\beta}|k|^\beta t^\alpha \big)$$

$$p(q,\bar{\Delta}) = E_\alpha\big(- D_{\alpha,\beta}\ |q|^\beta \bar{\Delta}^\alpha \big)$$

The α and the β enter into the expression in different ways, and hence can be measured separately!

Iso-b-value Diagram

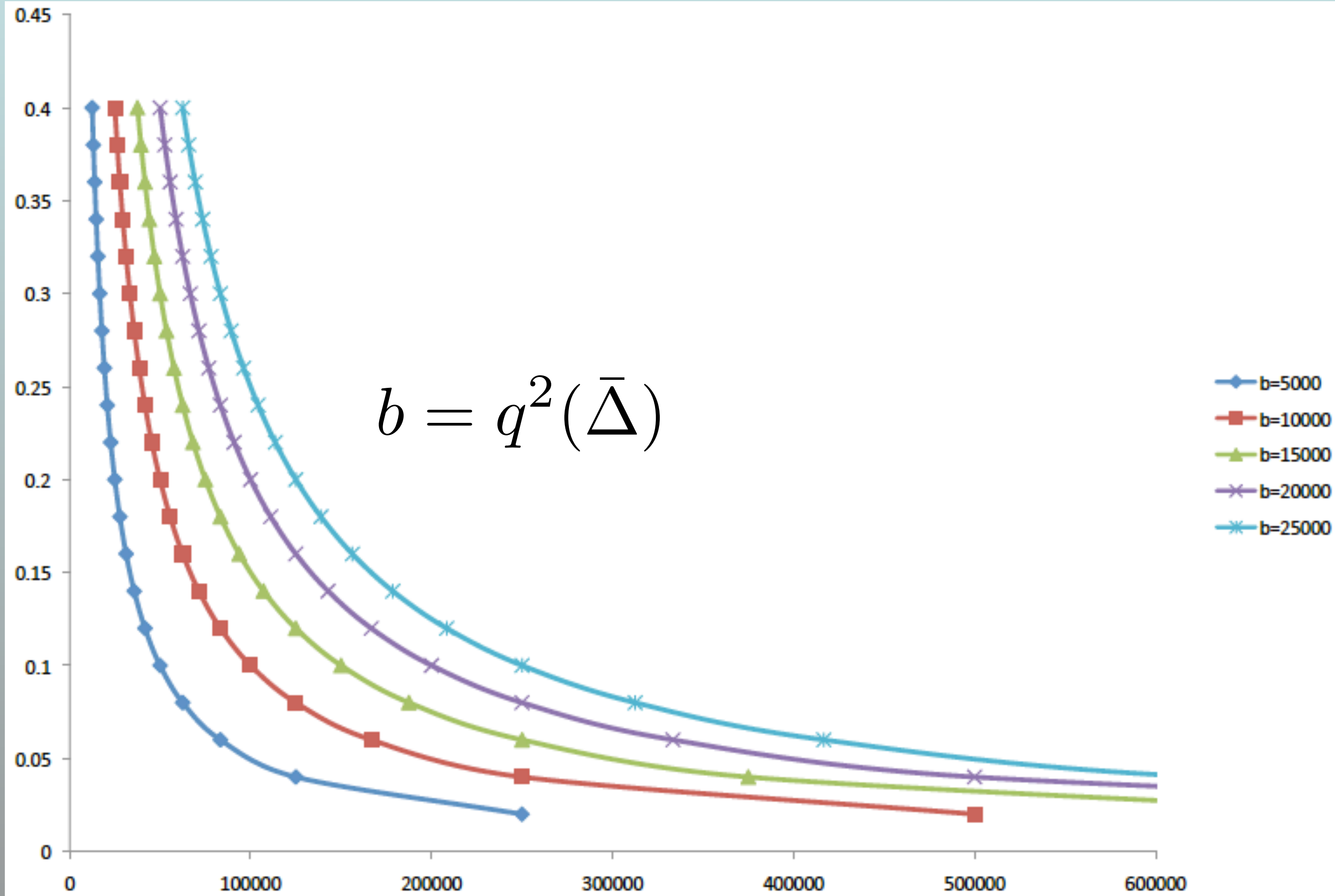

$\bar{\Delta}, seconds$

q^2, mm^{-2}

Iso-b-value Diagram

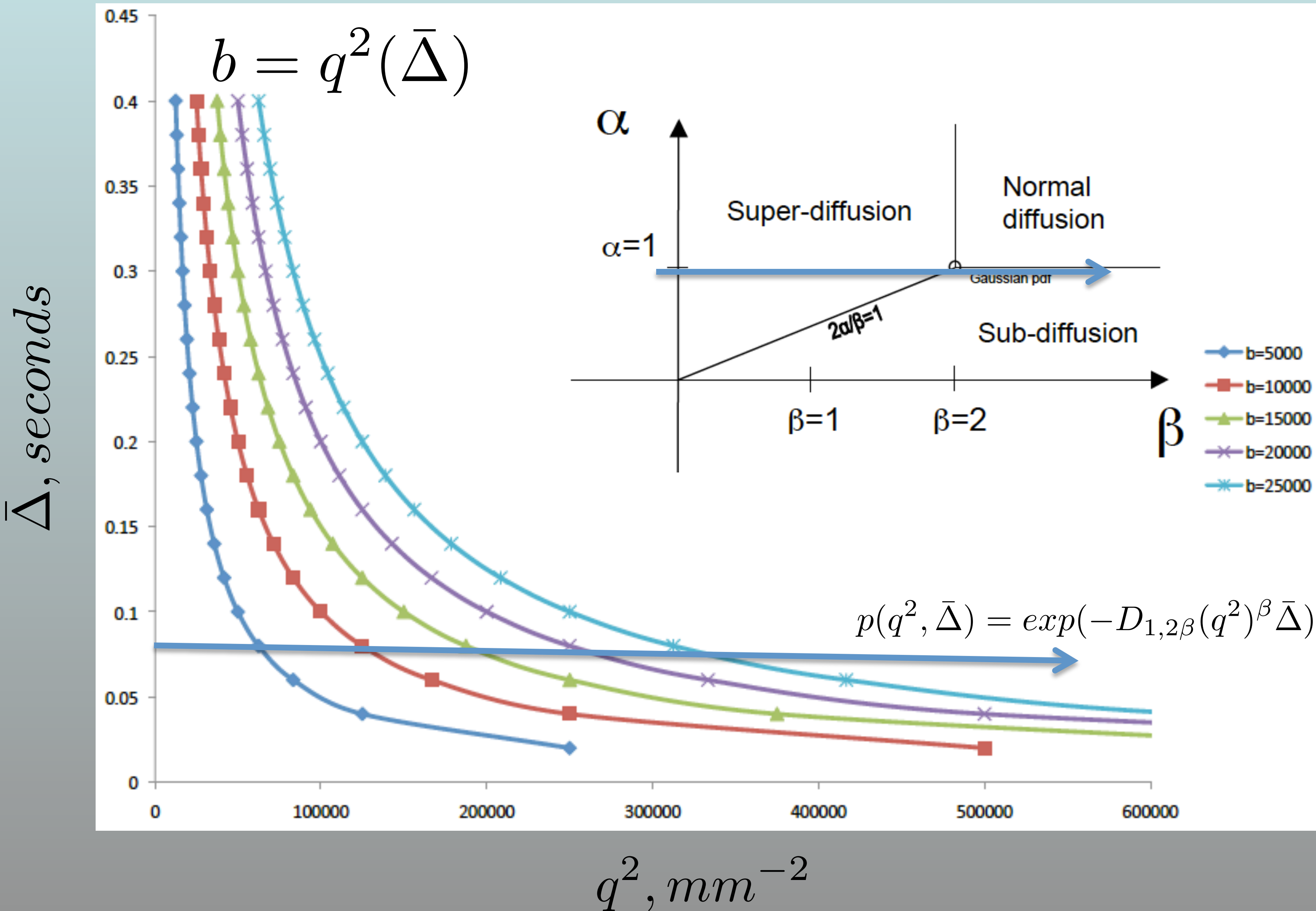

Iso-b-value Diagram

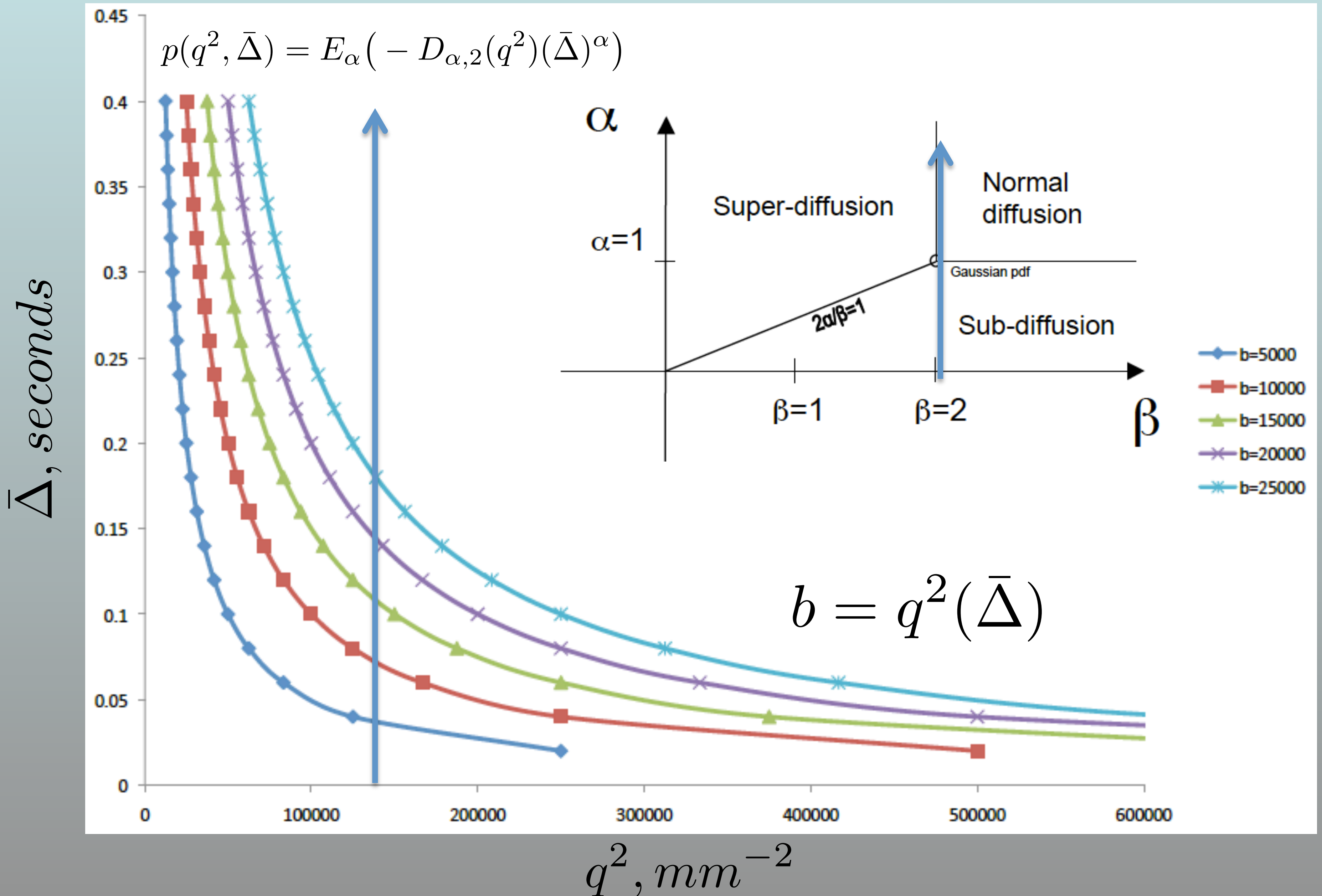

ROIs
(FOV 27 mm X 18 mm)

Cerebral Cortex (Grey Matter)

homogeneous & isotropic

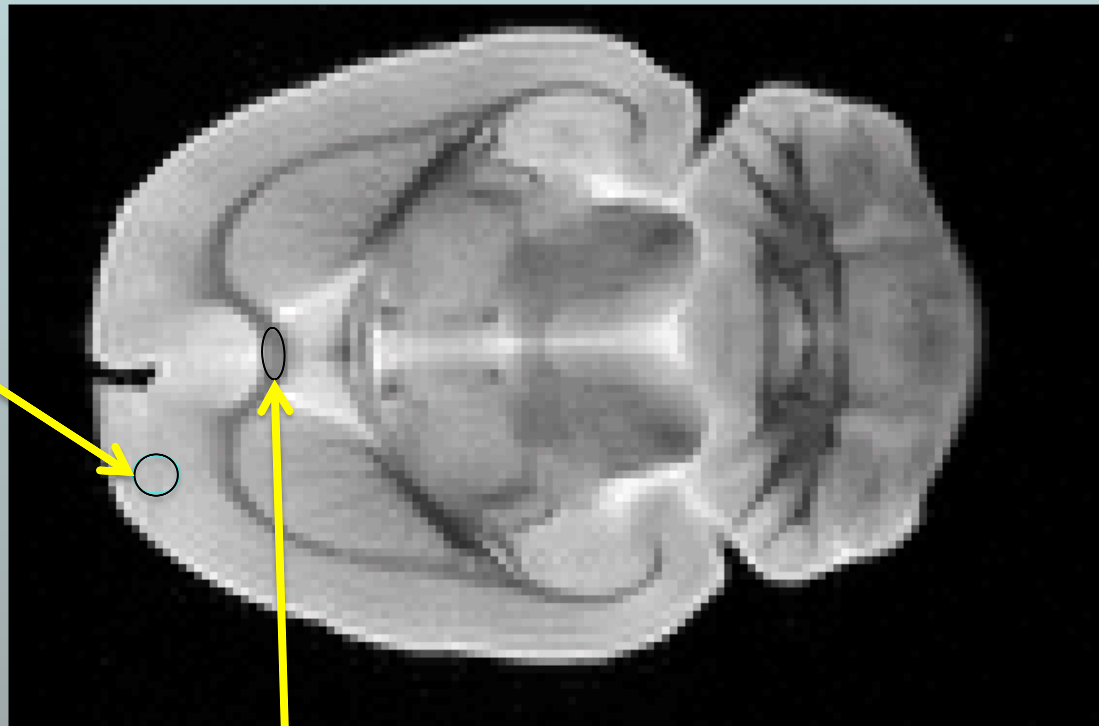

Corpus Callosum (White Matter)

heterogeneous, tortuous & anisotropic

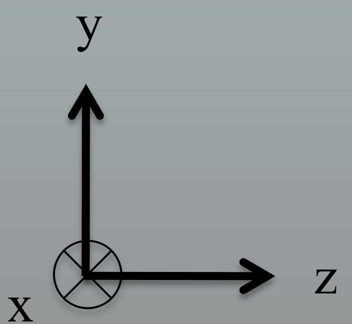

$$p(q,\bar{\Delta}) = E_\alpha\big(-D_{\alpha,\beta}|q|^\beta\bar{\Delta}^\alpha\big) \qquad \langle x^2(t)\rangle \sim t^{2\alpha/\beta}$$

parameter	Constant $\bar{\Delta}$ experiment
α	0.76 ± 0.05
β	1.95 ± 0.06
$2\alpha/\beta$	0.76 ± 0.08

GM

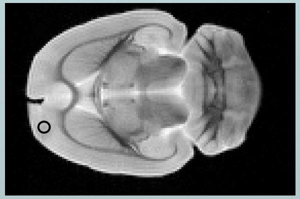

WM

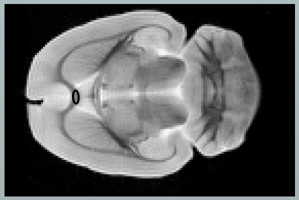

$$p(q,\bar{\Delta}) = E_\alpha\big(-D_{\alpha,\beta}|q|^\beta \bar{\Delta}^\alpha\big) \qquad \langle x^2(t)\rangle \sim t^{2\alpha/\beta}$$

parameter	Constant $\bar{\Delta}$ experiment
α	0.76 ± 0.05
β	1.95 ± 0.06
$2\alpha/\beta$	0.76 ± 0.08

GM

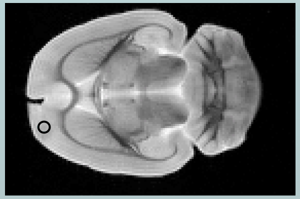

parameter	Constant q experiment
α	0.95 ± 0.01
β	1.91 ± 0.03
$2\alpha/\beta$	0.98 ± 0.02

WM

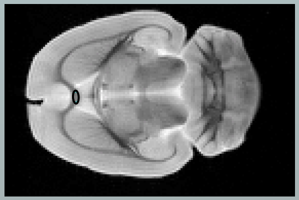

$$p(q, \bar{\Delta}) = E_\alpha\big(-D_{\alpha,\beta}|q|^\beta \bar{\Delta}^\alpha\big) \qquad \langle x^2(t)\rangle \sim t^{2\alpha/\beta}$$

parameter	Constant $\bar{\Delta}$ experiment
α	0.76 ± 0.05
β	1.95 ± 0.06
$2\alpha/\beta$	0.76 ± 0.08

GM

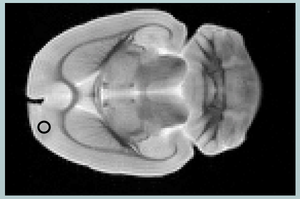

parameter	Constant q experiment
α	0.95 ± 0.01
β	1.91 ± 0.03
$2\alpha/\beta$	0.98 ± 0.02

parameter	Constant $\bar{\Delta}$ experiment
α	0.42 ± 0.04
β	1.15 ± 0.13
$2\alpha/\beta$	0.74 ± 0.12

WM

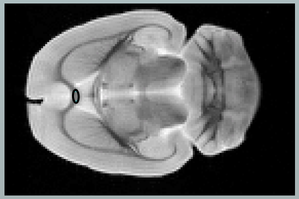

$$p(q,\bar{\Delta}) = E_\alpha\big(-D_{\alpha,\beta}|q|^\beta\bar{\Delta}^\alpha\big) \qquad \langle x^2(t)\rangle \sim t^{2\alpha/\beta}$$

GM

parameter	Constant $\bar{\Delta}$ experiment
α	0.76 ± 0.05
β	1.95 ± 0.06
$2\alpha/\beta$	0.76 ± 0.08

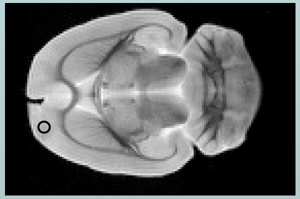

parameter	Constant q experiment
α	0.95 ± 0.01
β	1.91 ± 0.03
$2\alpha/\beta$	0.98 ± 0.02

WM

parameter	Constant $\bar{\Delta}$ experiment
α	0.42 ± 0.04
β	1.15 ± 0.13
$2\alpha/\beta$	0.74 ± 0.12

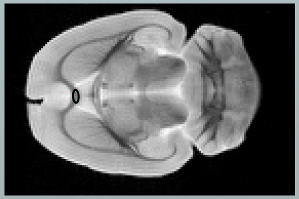

parameter	Constant q experiment
α	0.69 ± 0.05
β	1.85 ± 0.07
$2\alpha/\beta$	0.75 ± 0.05

$$p(q,\bar{\Delta}) = E_\alpha\big(-D_{\alpha,\beta}|q|^\beta\bar{\Delta}^\alpha\big) \qquad \langle x^2(t)\rangle \sim t^{2\alpha/\beta}$$

GM

parameter	Constant $\bar{\Delta}$ experiment
α	0.76 ± 0.05
β	1.95 ± 0.06
$2\alpha/\beta$	0.76 ± 0.08

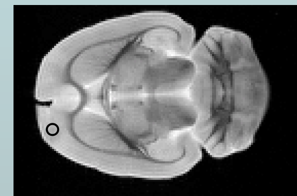

parameter	Constant q experiment
α	0.95 ± 0.01
β	1.91 ± 0.03
$2\alpha/\beta$	0.98 ± 0.02

WM

parameter	Constant $\bar{\Delta}$ experiment
α	0.42 ± 0.04
β	1.15 ± 0.13
$2\alpha/\beta$	0.74 ± 0.12

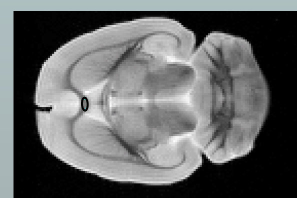

parameter	Constant q experiment
α	0.69 ± 0.05
β	1.85 ± 0.07
$2\alpha/\beta$	0.75 ± 0.05

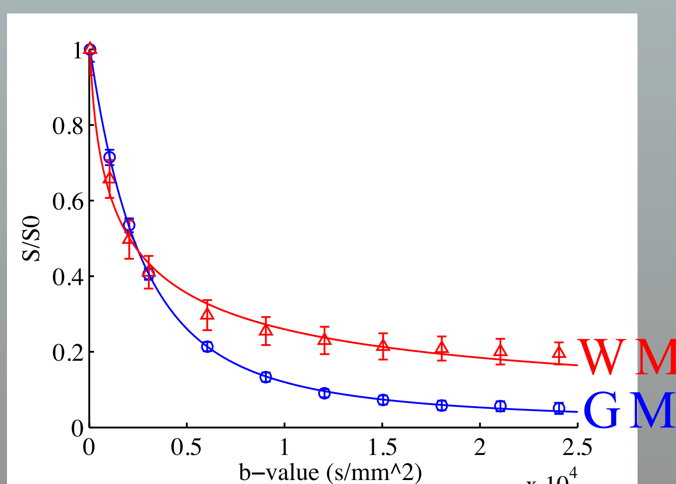

$$p(q, \bar{\Delta}) = E_\alpha\big(-D_{\alpha,\beta}|q|^\beta \bar{\Delta}^\alpha\big) \qquad \langle x^2(t)\rangle \sim t^{2\alpha/\beta}$$

parameter	Constant $\bar{\Delta}$ experiment
α	0.76 ± 0.05
β	1.95 ± 0.06
$2\alpha/\beta$	0.76 ± 0.08

GM

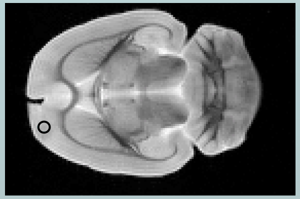

parameter	Constant q experiment
α	0.95 ± 0.01
β	1.91 ± 0.03
$2\alpha/\beta$	0.98 ± 0.02

parameter	Constant $\bar{\Delta}$ experiment
α	0.42 ± 0.04
β	1.15 ± 0.13
$2\alpha/\beta$	0.74 ± 0.12

WM

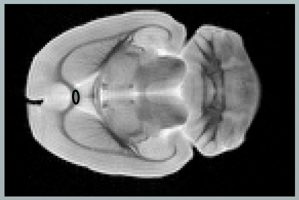

parameter	Constant q experiment
α	0.69 ± 0.05
β	1.85 ± 0.07
$2\alpha/\beta$	0.75 ± 0.05

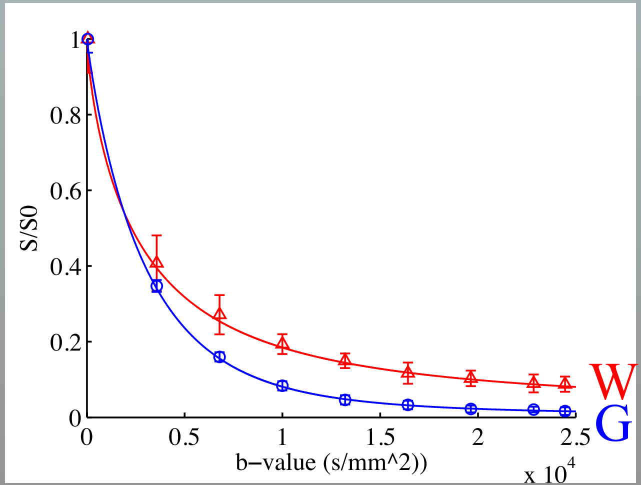

WM
GM

$$p(q,\bar{\Delta}) = E_\alpha\big(-D_{\alpha,\beta}|q|^\beta \bar{\Delta}^\alpha\big) \qquad \langle x^2(t)\rangle \sim t^{2\alpha/\beta}$$

GM

parameter	Constant $\bar{\Delta}$ experiment
α	0.76 ± 0.05
β	1.95 ± 0.06
$2\alpha/\beta$	0.76 ± 0.08

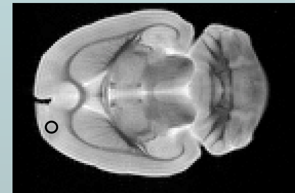

parameter	Constant q experiment
α	0.95 ± 0.01
β	1.91 ± 0.03
$2\alpha/\beta$	0.98 ± 0.02

WM

parameter	Constant $\bar{\Delta}$ experiment
α	0.42 ± 0.04
β	1.15 ± 0.13
$2\alpha/\beta$	0.74 ± 0.12

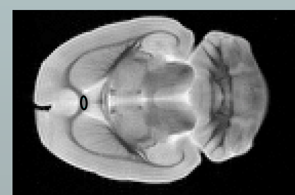

parameter	Constant q experiment
α	0.69 ± 0.05
β	1.85 ± 0.07
$2\alpha/\beta$	0.75 ± 0.05

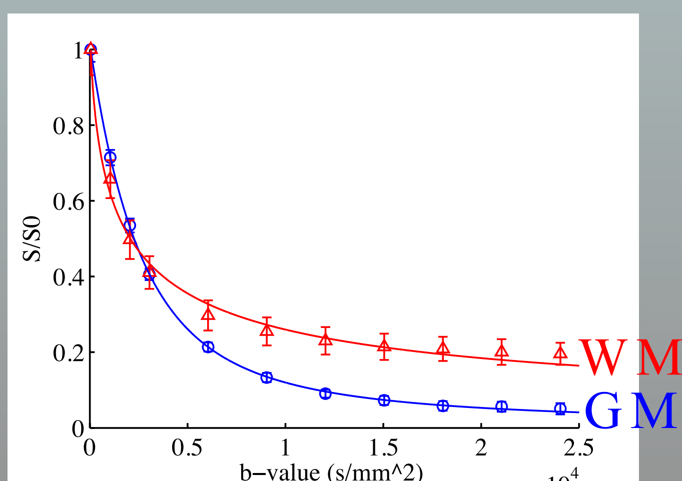

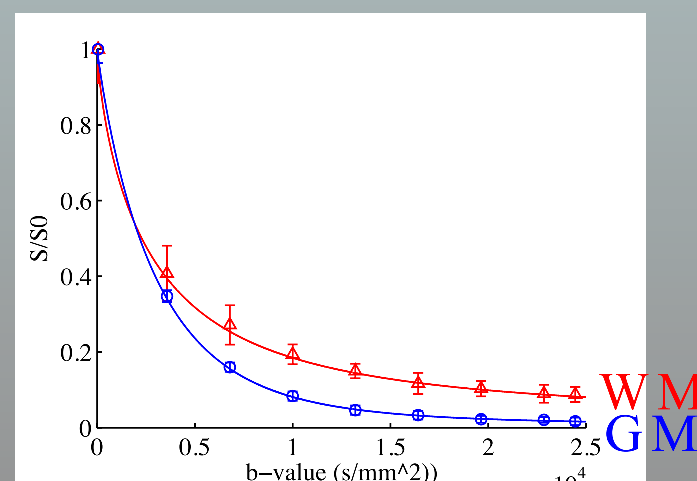

Parameter Maps

Constant $\bar{\Delta}$ experiment

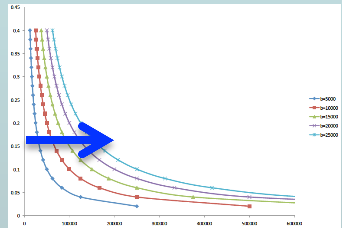

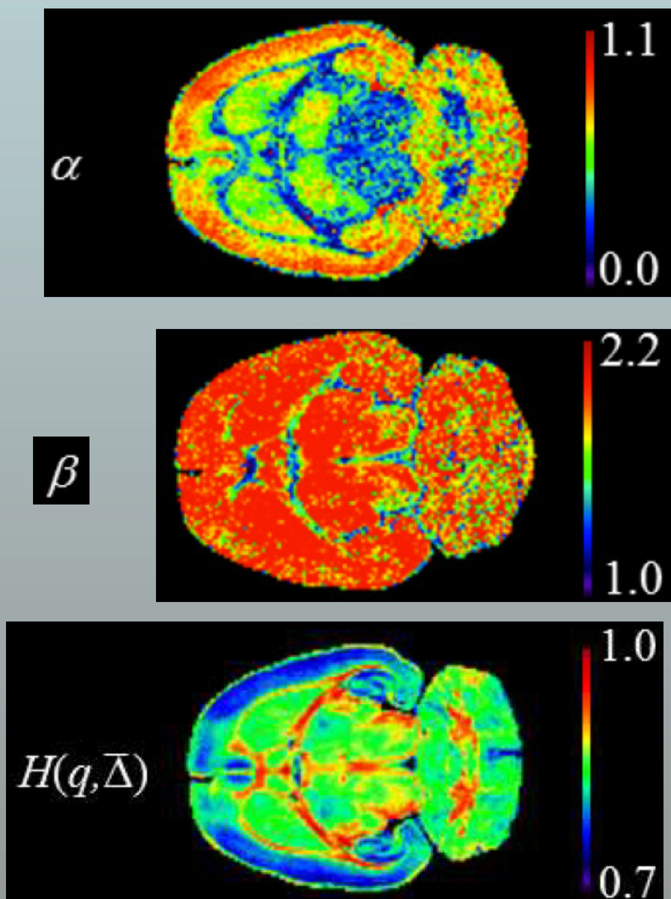

Parameter Maps

Constant $\bar{\Delta}$ experiment

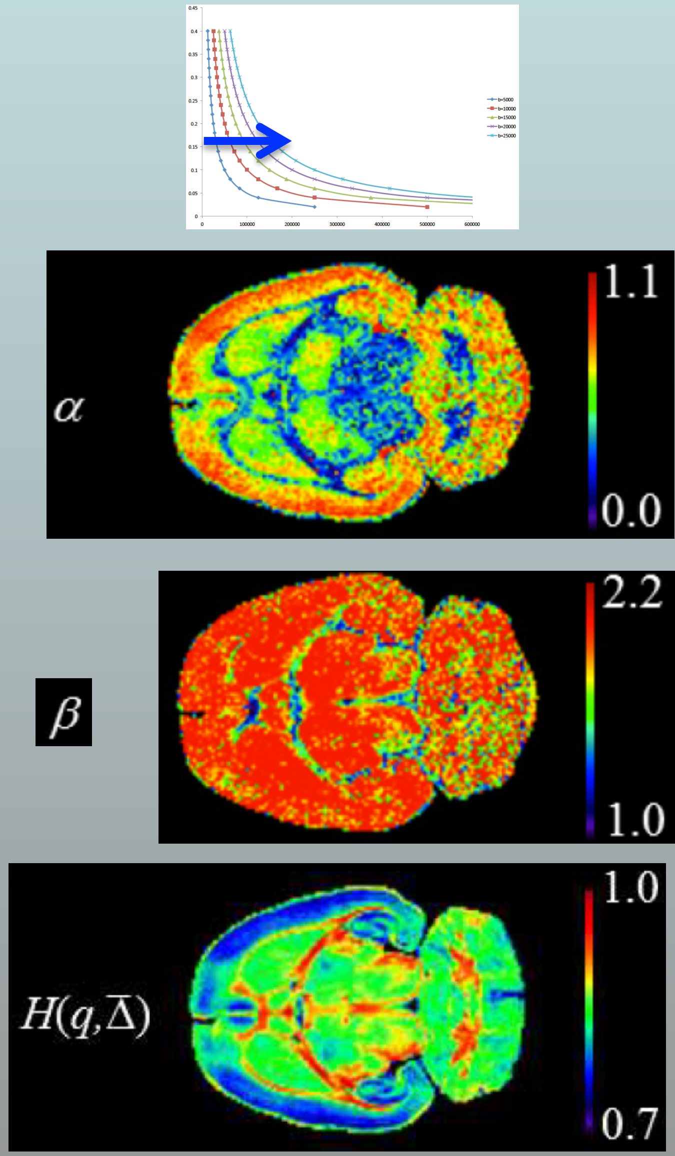

Constant q experiment

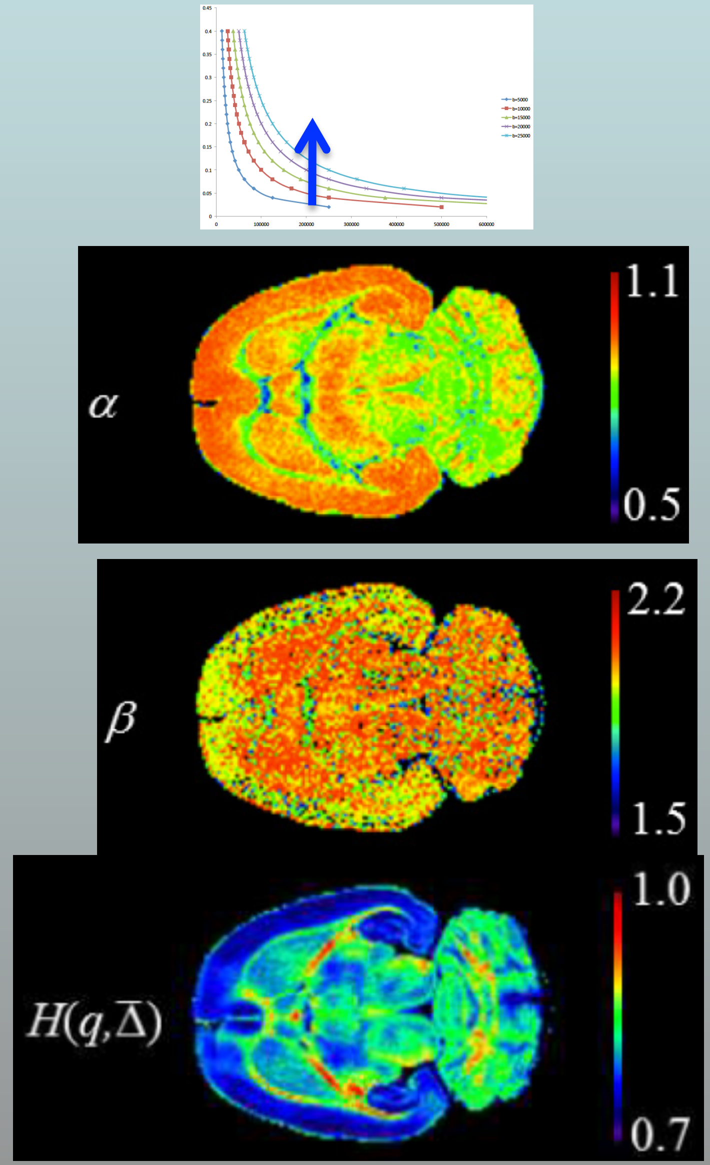

‘Information’ Gained by the MLF

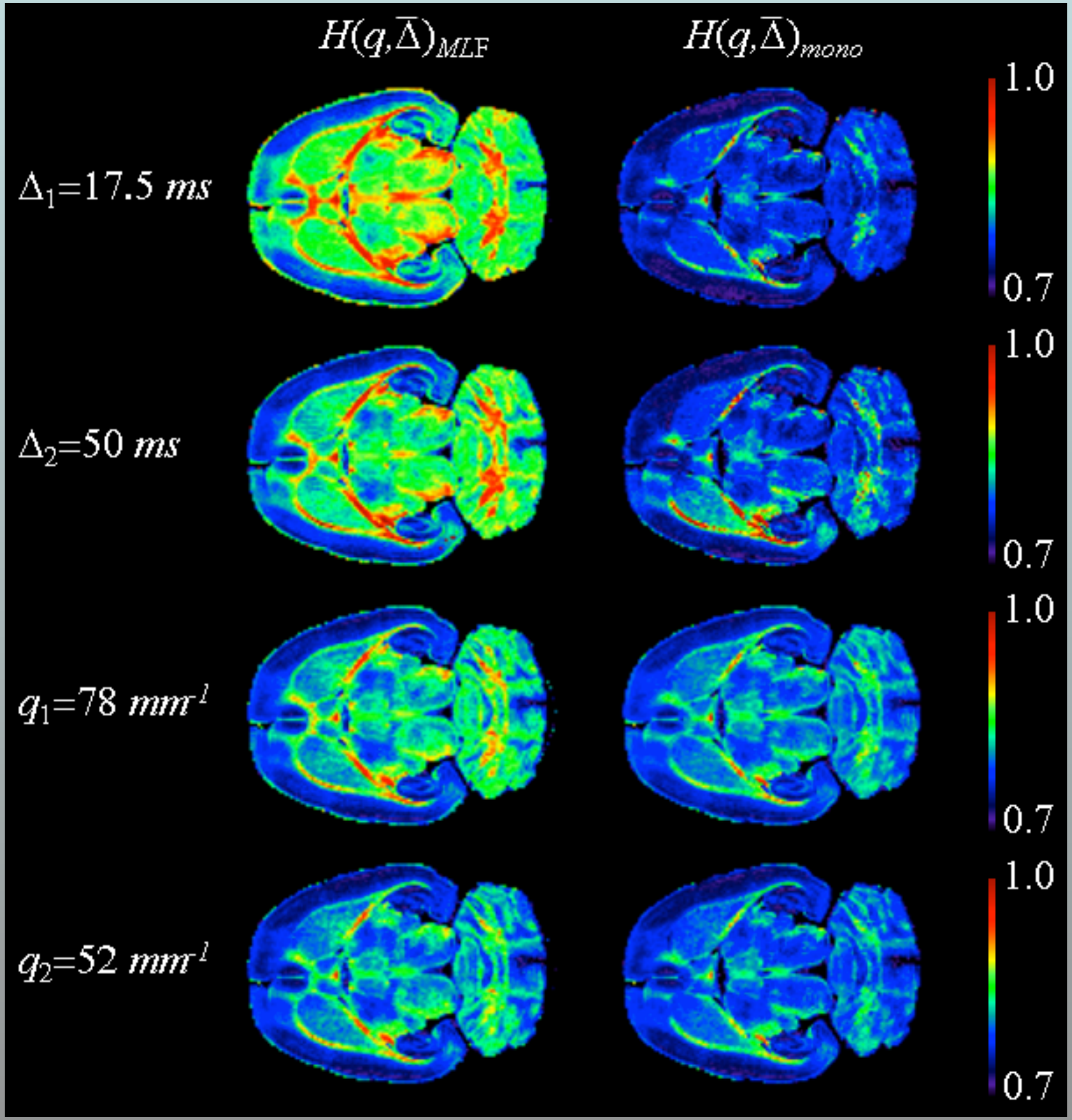

Fornix ROIs in Epileptic Subject

Mean and standard deviation of the MLF and entropy parameters for the fornix (F) ROIs in healthy and epileptic subjects in the constant $\Delta = 17.5\,ms$ experiments.

parameter	ROI	Healthy	Epileptic
α	F, left	0.25 ± 0.10	0.86 ± 0.09
	F, right	0.35 ± 0.11	0.84 ± 0.07
β	F, left	1.64 ± 0.23	1.92 ± 0.12
	F, right	1.44 ± 0.22	1.88 ± 0.11
$2\alpha/\beta$	F, left	0.33 ± 0.12	0.89 ± 0.05
	F, right	0.24 ± 0.13	0.88 ± 0.03
$H(q,\bar{\Delta})$	F, left	0.90 ± 0.08	0.56 ± 0.04
	F, right	0.91 ± 0.06	0.54 ± 0.05

Fractional anisotropy (FA) reduction of ~15% in fornix (Parekh et. al, *Exp Neurol*. 2010)

Fornix ROIs in Epileptic Subject

Mean and standard deviation of the MLF and entropy parameters for the fornix (F) ROIs in healthy and epileptic subjects in the constant $\Delta = 17.5\,ms$ experiments.

parameter	ROI	Healthy	Epileptic
α	F, left	0.25 ± 0.10	0.86 ± 0.09
	F, right	0.35 ± 0.11	0.84 ± 0.07
β	F, left	1.64 ± 0.23	1.92 ± 0.12
	F, right	1.44 ± 0.22	1.88 ± 0.11
$2\alpha/\beta$	F, left	0.33 ± 0.12	0.89 ± 0.05
	F, right	0.24 ± 0.13	0.88 ± 0.03
$H(q,\bar{\Delta})$	F, left	0.90 ± 0.08	0.56 ± 0.04
	F, right	0.91 ± 0.06	0.54 ± 0.05

Fractional anisotropy (FA) reduction of ~15% in fornix (Parekh et. al, *Exp Neurol*. 2010)

Fornix ROIs in Epileptic Subject

Mean and standard deviation of the MLF and entropy parameters for the fornix (F) ROIs in healthy and epileptic subjects in the constant $\Delta = 17.5\,ms$ experiments.

parameter	ROI	Healthy	Epileptic
α	F, left	0.25 ± 0.10	0.86 ± 0.09
	F, right	0.35 ± 0.11	0.84 ± 0.07
β	F, left	1.64 ± 0.23	1.92 ± 0.12
	F, right	1.44 ± 0.22	1.88 ± 0.11
$2\alpha/\beta$	F, left	0.33 ± 0.12	0.89 ± 0.05
	F, right	0.24 ± 0.13	0.88 ± 0.03
$H(q,\bar{\Delta})$	F, left	0.90 ± 0.08	0.56 ± 0.04
	F, right	0.91 ± 0.06	0.54 ± 0.05

Fractional anisotropy (FA) reduction of ~15% in fornix (Parekh et. al, *Exp Neurol*. 2010)

Fornix ROIs in Epileptic Subject

Mean and standard deviation of the MLF and entropy parameters for the fornix (F) ROIs in healthy and epileptic subjects in the constant $\Delta = 17.5\,ms$ experiments.

parameter	ROI	Healthy	Epileptic
α	F, left	0.25 ± 0.10	0.86 ± 0.09
	F, right	0.35 ± 0.11	0.84 ± 0.07
β	F, left	1.64 ± 0.23	1.92 ± 0.12
	F, right	1.44 ± 0.22	1.88 ± 0.11
$2\alpha/\beta$	F, left	0.33 ± 0.12	0.89 ± 0.05
	F, right	0.24 ± 0.13	0.88 ± 0.03
$H(q, \bar{\Delta})$	F, left	0.90 ± 0.08	0.56 ± 0.04
	F, right	0.91 ± 0.06	0.54 ± 0.05

Fractional anisotropy (FA) reduction of ~15% in fornix (Parekh et. al, *Exp Neurol*. 2010)

Brain MRI at 3 T

Fractional Order Parameter Maps

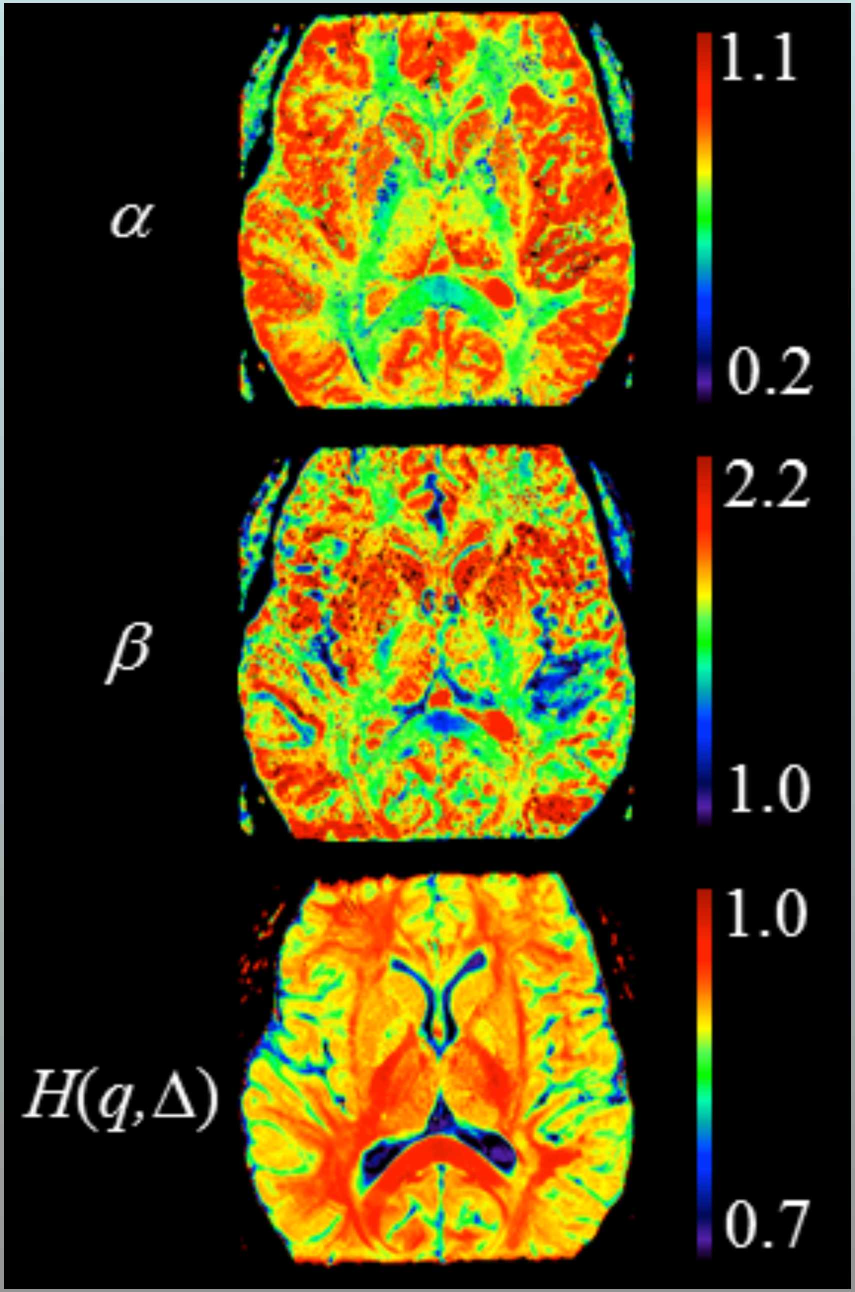

Courtesy
of
Thomas
Barrick

ROIs

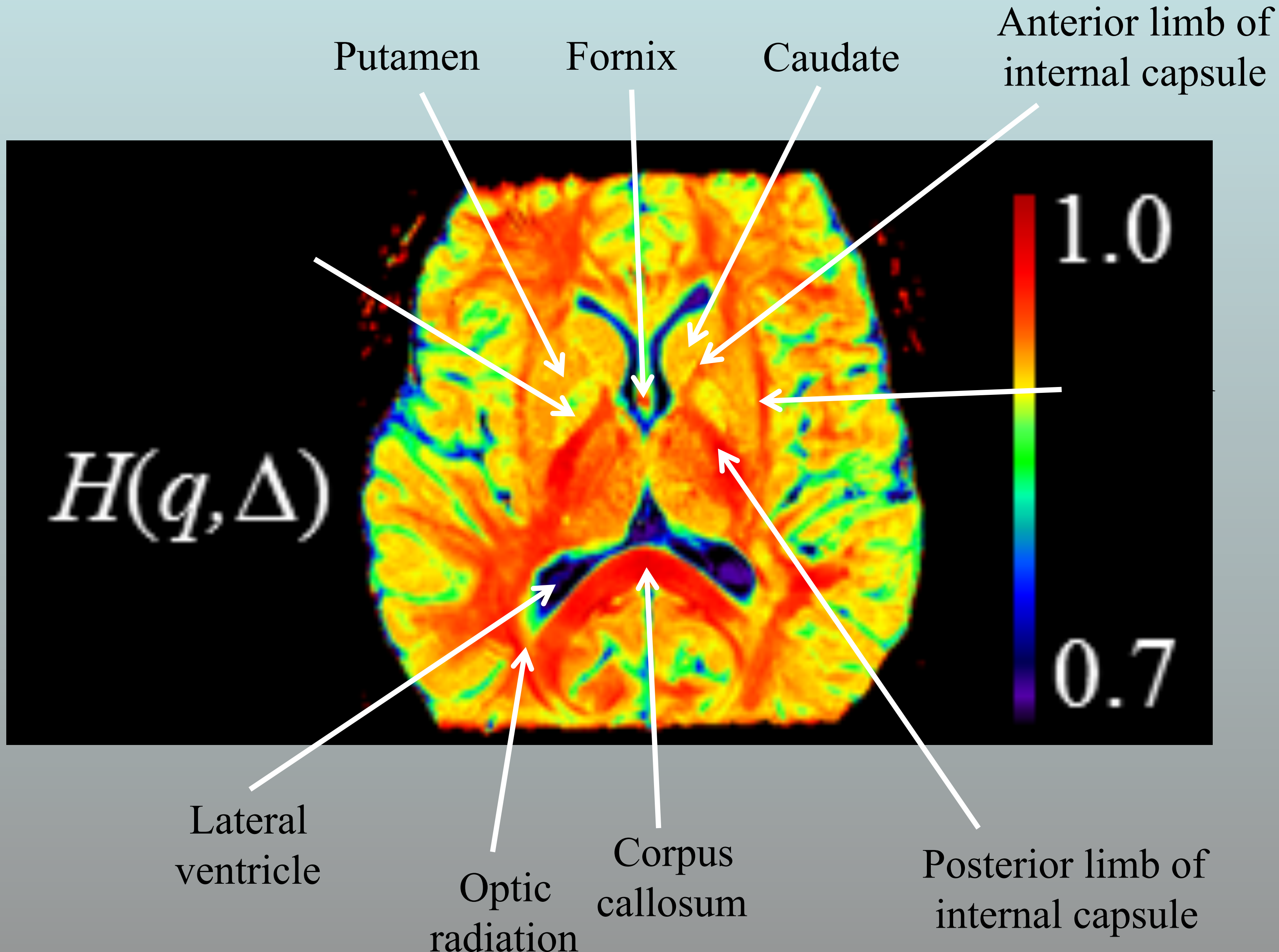
Putamen
Fornix
Caudate
Anterior limb of internal capsule
1.0
$H(q,\Delta)$
0.7
Lateral ventricle
Optic radiation
Corpus callosum
Posterior limb of internal capsule

Human Connectome Project (HCP)

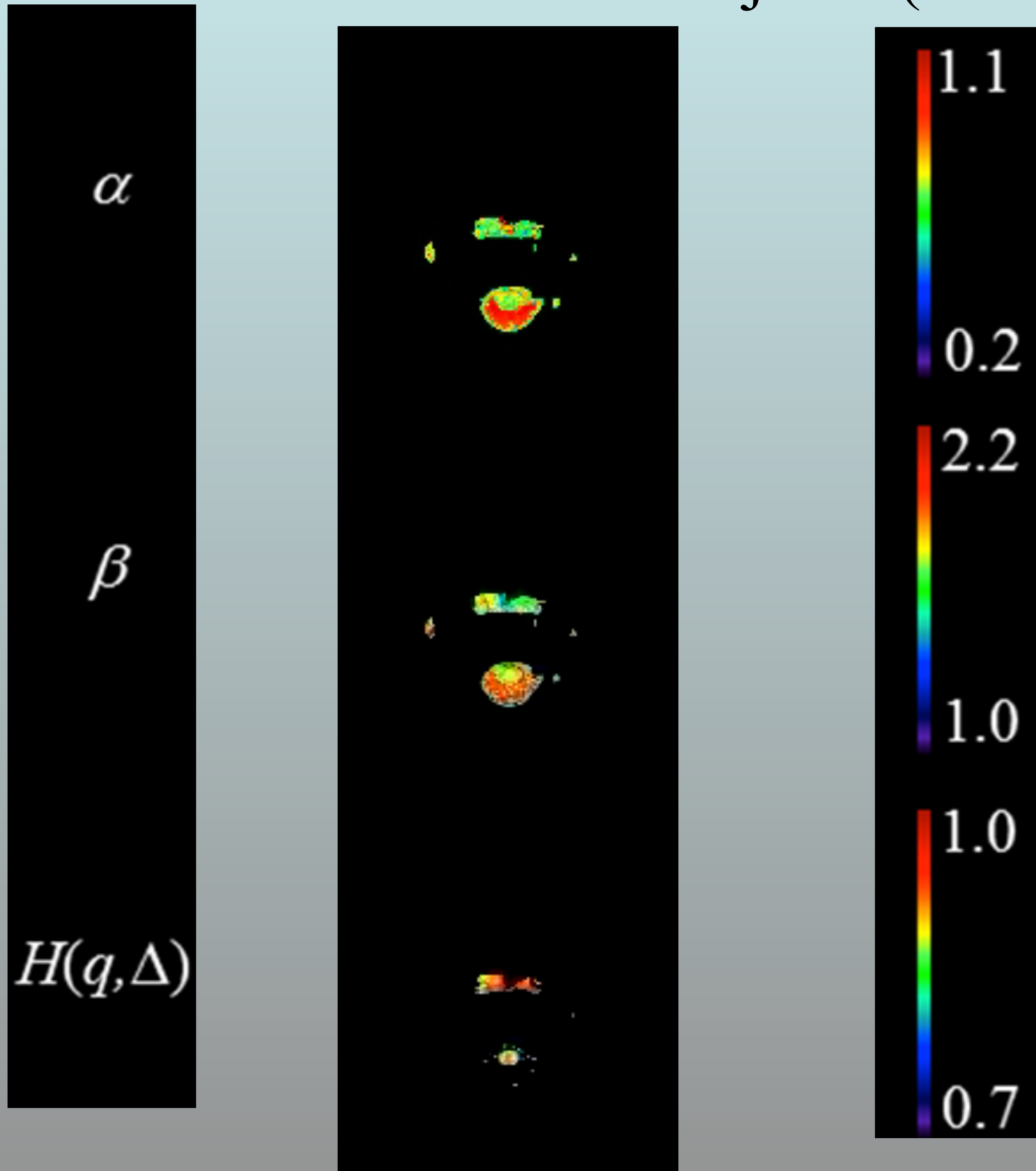

Courtesy of Thomas Barrick

Entropy of CSF

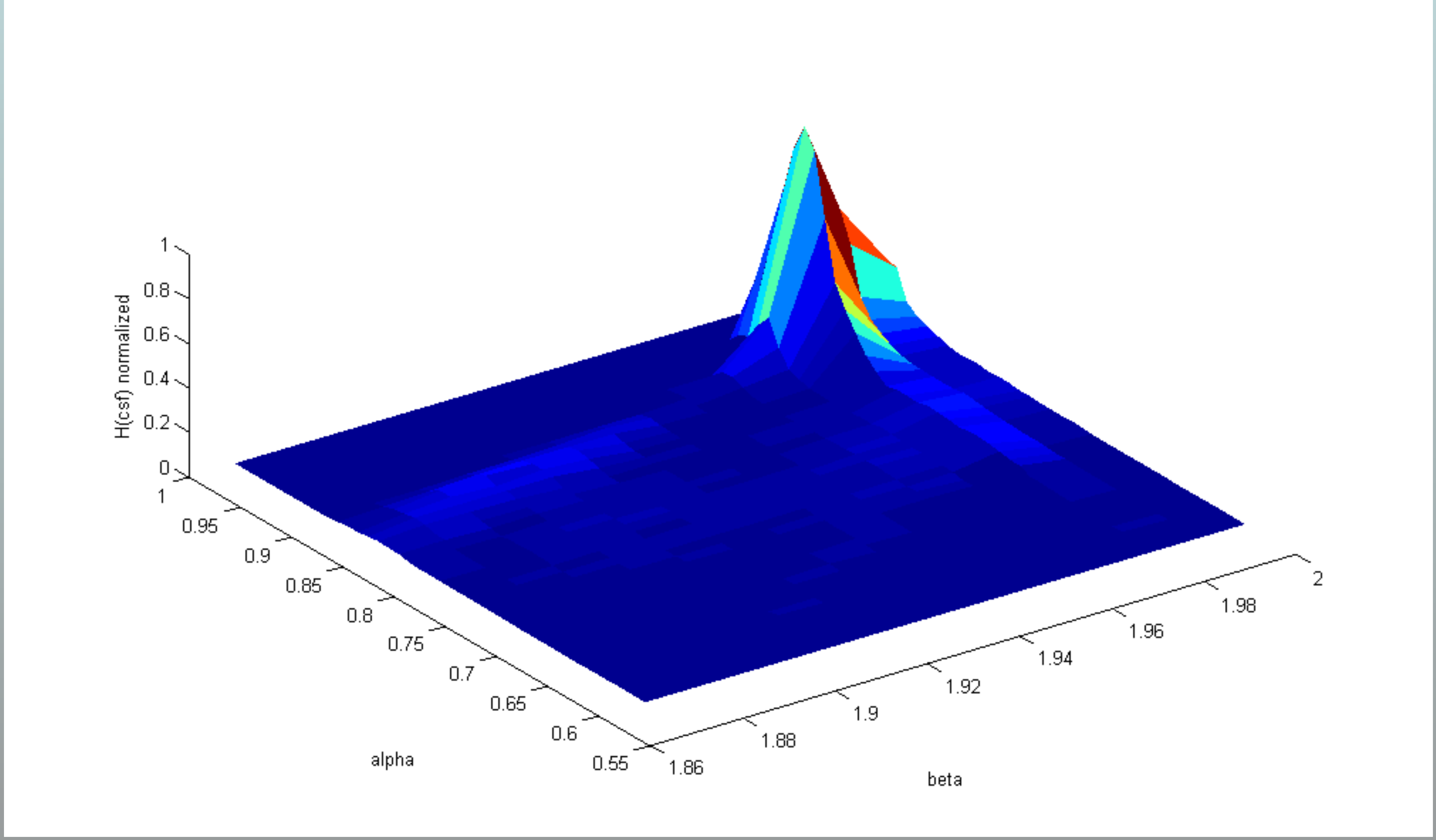

Entropy of Gray Matter

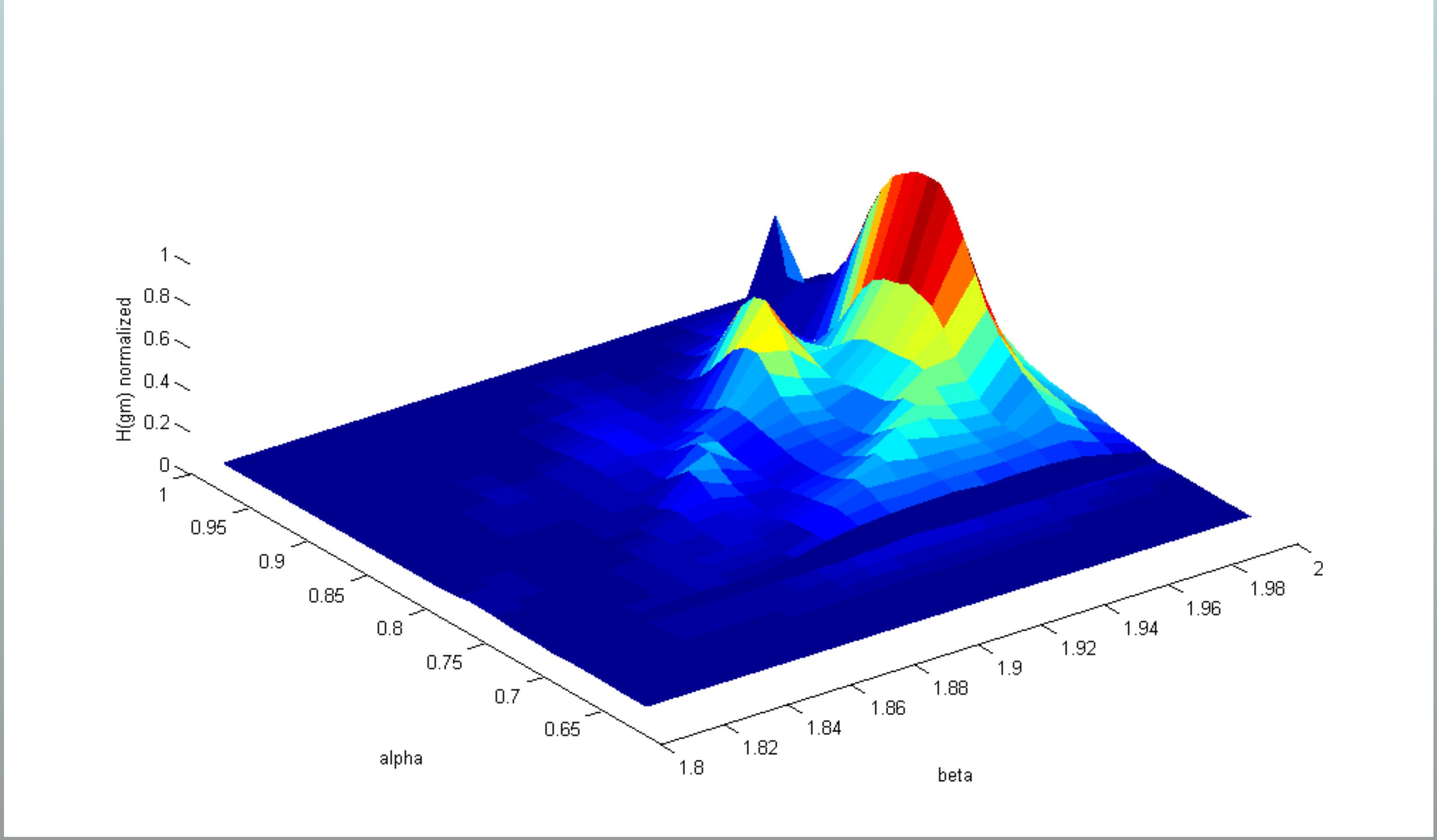

Entropy of White Matter

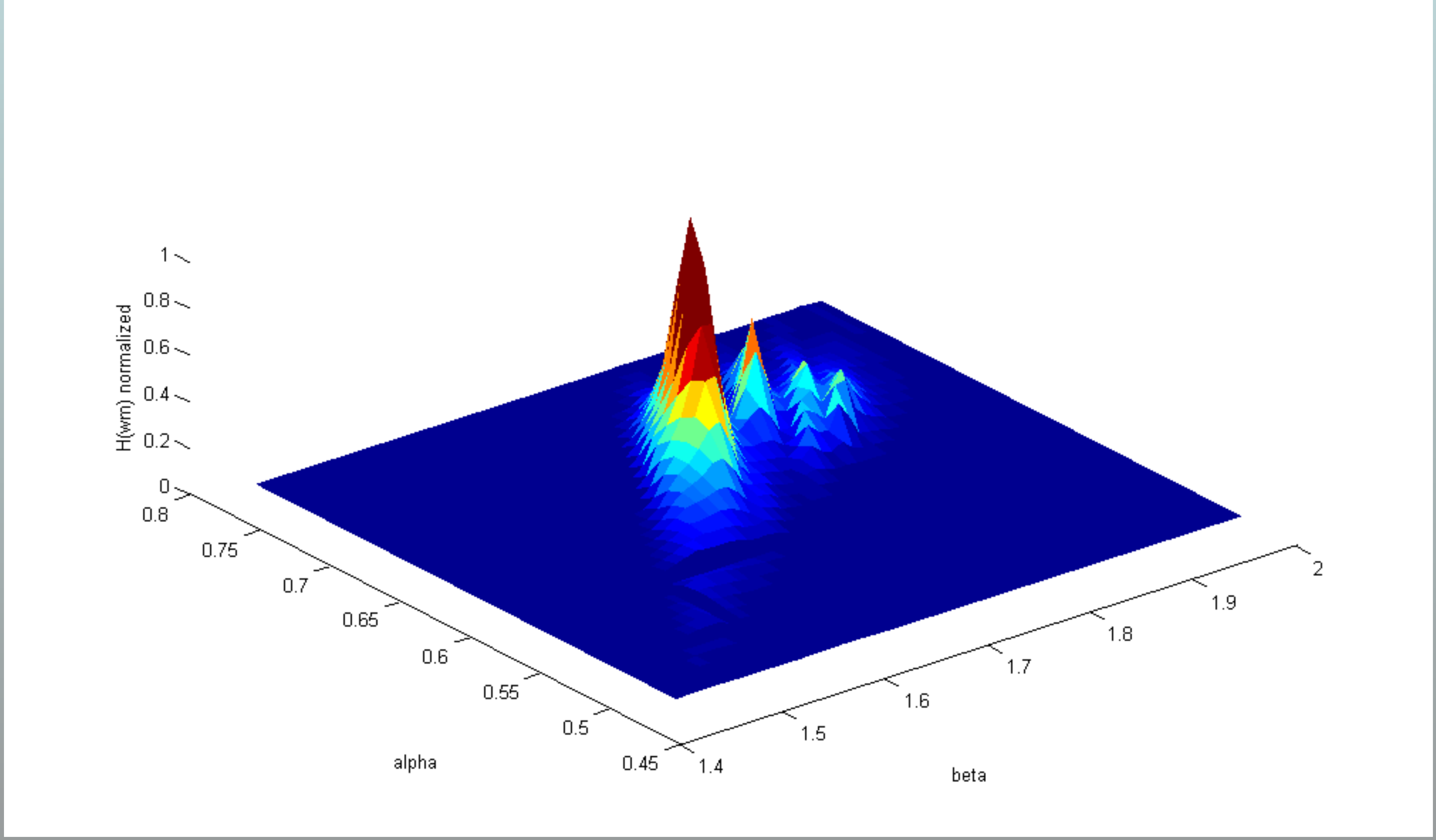

Conclusions & Future Work

- A *b*-value isn't *just* a *b*-value (weighting *q* vs. Δ) – tempered distributions?
- α, β and entropy (H) provide 'information' about the diffusion dynamics within the tissue microstructure
- Neurodegenerative disease models (PTU)
- Clinical implementation
- Biomarkers for changes in brain structure?

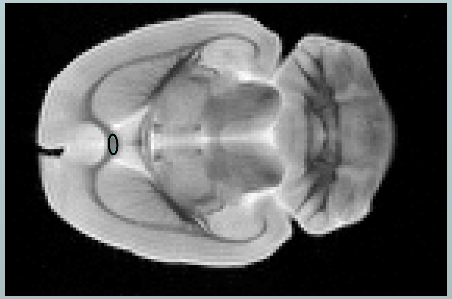

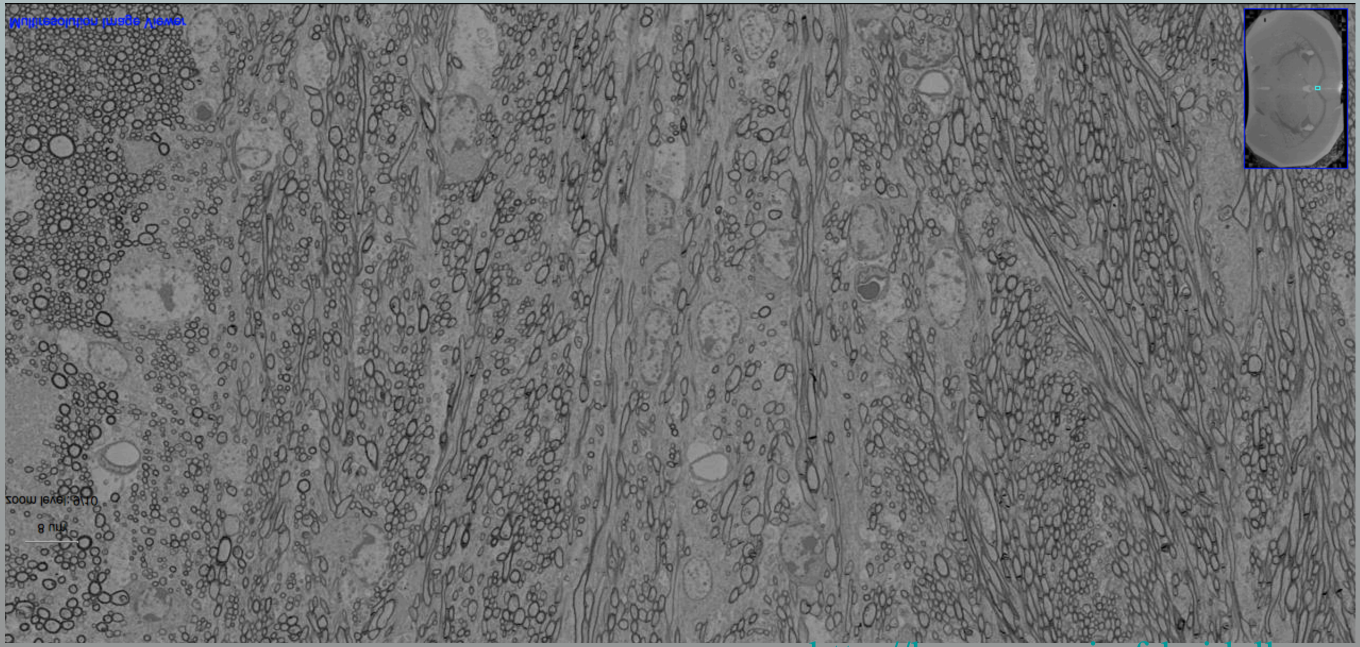

http://homes.mpimf-heidelberg.mpg.de/~smikula/

Acknowledgements

Thomas Barrick, St. Georges, University of London

Matt Hall, University College, London

Xiaohong Joe Zhou, UIC MRI Center

Yi Sui, UIC, BioE, UIC

Dan Plant, AMRIS, University of Florida

Recent NMR and FC Papers

R.L. Magin, O. Abdullah, D. Baleanu, and X.J. Zhou, Anomalous diffusion expressed through fractional order differential operators in the Bloch-Torrey equation, *Journal of Magnetic Resonance*, vol. 190, pp. 255-270, 2008.

R.L. Magin, X. Feng, and D. Baleanu, Fractional calculus in NMR, *Magnetic Resonance Engineering*, vol. 34, pp. 16-23, 2009.

X.J. Zhou, Q. Gao, O. Abdullah, and R.L. Magin, Studies of anomalous diffusion in the human brain using fractional order calculus, *Magnetic Resonance in Medicine*, vol. 63, pp. 562-569, 2010.

Q. Gao, G. Srinivasan, R.L. Magin, and X.J. Zhou, Anomalous diffusion measured by a twice-refocused spin echo pulse sequence: Analysis using fractional order calculus, *Journal of Magnetic Resonance Imaging*, vol. 33, pp. 1177-1183, 2011.

R.L. Magin, W. Li, M.P. Velasco, J. Trujillo, D.A. Reiter, A. Morgenstern, and R.G. Spencer, Fractional-Order models of anomalous NMR relaxation in cartilage matrix components and native cartilage, *Journal of Magnetic Resonance*, vol. 210, pp. 184-191, 2011.

Hanyga and M. Seredynska, Anisotropy in high-resolution diffusion-weighted MRI and anomalous diffusion, *Journal of Magnetic Resonance*, vol. 220, pp. 85-93, 2012.

C. Ingo, R.L. Magin, L. Colon-Perez, W. Triplett, and T.H. Mareci, Random walks and entropy in diffusion weighted magnetic resonance imaging studies of neural tissue, *Magnetic Resonance in Medicine*, (in press).

R. L. Magin, C. Ingo, L. Colon-Perez, W. Triplett, and T.H. Mareci, "Characterization of anomalous diffusion in porous biological tissues using fractional order derivatives and entropy," *Microporous and Mesoporous Materials*, (in press).

Théorie Analytique de la Chaleur,1822

Joseph Fourier

1768 -1830 - 2013

Preliminary Discourse

"After having established these differential equations their integrals must be obtained; this process consists in passing from a common expression to a particular solution subject to all the given conditions."

"The method which is derived from them leaves nothing vague and indeterminate in the solutions, it leads them up to the final numerical applications, a necessary condition of every investigation, without which we should only arrive at useless transformations."

Let *v* be the actual temperature of the point (*x,y,z*). The following equation represents the movement of heat in the interior of bodies.

$$\frac{d^{\alpha} v}{dt^{\alpha}} = \frac{K_{\alpha,\beta}}{CD}\left(\frac{d^{\beta} v}{dx^{\beta}} + \frac{d^{\beta} v}{dy^{\beta}} + \frac{d^{\beta} v}{dz^{\beta}}\right)$$

$K_{\alpha,\beta}$ – thermal conductivity
C – specific heat
D – density

Théorie Analytique de la Chaleur,1822

Preliminary Discourse

"After having established these differential equations their integrals must be obtained; this process consists in passing from a common expression to a particular solution subject to all the given conditions."

"The method which is derived from them leaves nothing vague and indeterminate in the solutions, it leads them up to the final numerical applications, a necessary condition of every investigation, without which we should only arrive at useless transformations."

Joseph Fourier

1768 -1830 - 2013

Let *v* be the actual temperature of the point (*x,y,z*). The following equation represents the movement of heat in the interior of bodies.

$$\frac{d^\alpha v}{dt^\alpha} = \frac{K_{\alpha,\beta}}{CD}\left(\frac{d^\beta v}{dx^\beta} + \frac{d^\beta v}{dy^\beta} + \frac{d^\beta v}{dz^\beta}\right)$$

$K_{\alpha,\beta}$ – thermal conductivity
C – specific heat
D – density

Linear and Complex Systems